Time-dependent scale-free brain dynamics during naturalistic inputs

Philipp Klar, Yasir Çatal, Gerhard Jocham, Robert Langner, Georg Northoff

Suggested Citation:
Klar, P., Çatal, Y., Jocham, G., Langner, R., & Northoff, G. (2025). Time-dependent scale-free brain dynamics during naturalistic inputs. NeuroImage, 314, Article 121255.
https://doi.org/10.1016/j.neuroimage.2025.121255

NeuroImage 314 (2025) 121255

Contents lists available at ScienceDirect

NeuroImage

journal homepage: www.elsevier.com/locate/ynimg

Time-dependent scale-free brain dynamics during naturalistic inputs

Philipp Klar[a,b,*], Yasir Çatal[c], Gerhard Jocham[a], Robert Langner[b,d], Georg Northoff[e]

[a] Faculty of Mathematics and Natural Sciences, Institute of Experimental Psychology, Heinrich Heine University of Düsseldorf, Düsseldorf, Germany
[b] Institute of Neuroscience and Medicine, Brain & Behaviour (INM-7), Research Centre Jülich, Jülich, Germany
[c] The Royal's Institute of Mental Health Research & University of Ottawa. Brain and Mind Research Institute, Centre for Neural Dynamics, Faculty of Medicine, University of Ottawa, 145 Carling Avenue, Rm. 6435, Ottawa, Ontario K1Z 7K4, Canada
[d] Institute of Systems Neuroscience, Heinrich Heine University Düsseldorf, Düsseldorf, Germany
[e] University of Ottawa, Institute of Mental Health Research at the Royal Ottawa Hospital, 145 Carling Avenue, Rm. 6435, Ottawa, Ontario K1Z 7K4, Canada

ARTICLE INFO

Keywords:
Fractal dynamics
Scale-free dynamics
Spectral exponent
Inter-subject correlation
ISC

ABSTRACT

Environmental processes, such as auditory and visual inputs, often follow power-law distributions with a time-dependent and constantly changing spectral exponent, β(t). However, it remains unclear how the brain's scale-free dynamics continuously respond to naturalistic inputs, such as by potentially alternating instead of static levels of the spectral exponent. Our fMRI study investigates the brain's dynamic, time-dependent spectral exponent, β(t), during movie-watching, and uses time-varying inter-subject correlation, ISC(t), to assess the extent to which input dynamics are reflected as shared brain activity across subjects in early sensory regions. Notably, we investigate the level of ISC particularly based on the modulation by time-dependent scale-free dynamics or β(t). We obtained three key findings: First, the brain's β(t) showed a distinct temporal structure in visual and auditory regions during naturalistic inputs compared to the resting-state, investigated in the 7 Tesla Human Connectome Project dataset. Second, β(t) and ISC(t) were positively correlated during naturalistic inputs. Third, grouping subjects based on the Rest-to-Movie standard deviation change of the time-dependent spectral exponent β(t) revealed that the brain's relative shift from intrinsic to stimulus-driven scale-free dynamics modulates the level of shared brain activity, or ISC(t), and thus the imprinting of inputs on brain activity. This modulation was further supported by the observation that the two groups displayed significantly different β(t)-ISC(t) correlations, where the group with a higher mean of ISC(t) during inputs also exhibited a higher β(t)-ISC(t) correlation in visual and auditory regions. In summary, our fMRI study underscores a positive relationship between time-dependent scale-free dynamics and ISC, where higher spectral exponents correspond to higher degrees of shared brain activity during ongoing audiovisual inputs.

1. Introduction

The environment continuously bombards the human brain with fluctuating auditory and visual inputs. To process these inputs, the brain aligns its ongoing intrinsic spontaneous activity with the dynamics of sensory inputs, enabling the perception of the world around us. A closer examination of auditory and visual inputs reveals that natural phenomena often exhibit fractal or scale-free dynamics (Bak, 1996; Mandelbrot, 1999; Schroeder, 2009). A scale-free process is characterized by a power spectrum that follows a power-law distribution on a log-frequency versus log-power plot. This type of distribution is commonly referred to as a 1/f distribution, since power gradually decreases (or rarely increases) as frequency increases, without a dominant frequency, hence the term "scale-free" (Schroeder, 2009). The spectral slope or exponent (β) can be measured by fitting a linear regression to the log-frequency and log-power values (Bak, 1996; Mandelbrot, 1999; Schroeder, 2009).

Examples of auditory phenomena that exhibit scale-free dynamics cover human speech (Sabanal and Nakagawa, 1996; Luque et al., 2015) and music across various genres (Voss and Clarke, 1975; Voss and Clarke, 1978; Hsü and Hsü, 1991; Su and Wu, 2007; Levitin et al., 2012; González-Espinoza et al., 2017). Visual phenomena, such as natural scenes and images, also display scale-free temporal and spatial properties (Field, 1987; Nyikos et al., 1994; Field and Graham, 2007; Forsythe et al., 2011). Scale-free dynamics are not limited to natural phenomena; even human creations or artifacts, like modern movies, can exhibit

---

* Corresponding author.
E-mail address: philipp.klar@hhu.de (P. Klar).

https://doi.org/10.1016/j.neuroimage.2025.121255
Received 5 August 2024; Received in revised form 20 January 2025; Accepted 8 May 2025

audiovisual properties, such as scene lengths, that follow a scale-free distribution over time (Cutting et al., 2010; Cutting et al., 2012; Cutting et al., 2018). Given the pervasive presence of scale-free dynamics in environmental sensory inputs, the central question of our functional magnetic resonance imaging (fMRI) study is: how do the brain's scale-free dynamics in auditory and visual regions continuously respond in a time-dependent manner to naturalistic, ongoing inputs that often exhibit scale-free properties themselves?

Turning from the scale-free dynamics of sensory and naturalistic inputs to the brain, a large body of electrophysiological and fMRI studies has demonstrated that human brain activity can also exhibit scale-free dynamics. This occurs both in the brain's ongoing spontaneous activity during resting-state conditions and in response to stimuli during task states (He et al., 2010; Kasagi et al., 2017; Huang et al., 2017; Campbell and Weber, 2022; Campbell et al., 2022; Wainio-Theberge et al., 2022; Klar et al., 2023a; Klar et al., 2023b; Grosu et al., 2023). Neuroimaging findings have shown that scale-free neuronal dynamics optimize the brain's responsiveness to, and processing of, sensory inputs (Gervais et al., 2023). Studies also demonstrated that the brain's scale-free dynamics, as measured by the spectral exponent β, can systematically increase or decrease in response to different types of event-related designs. In fast event-related designs, power is transiently shifted from slower to faster frequencies (He, 2011; Kasagi et al., 2017; Wainio-Theberge et al., 2022). Conversely, in slow event-related designs, β can increase since power shifts from faster to slower frequencies (Klar et al., 2023a; Klar et al., 2023b). Event-related studies typically focus on the brain's reactivity to temporally discontinuous or chopped-up inputs in time, which are often analyzed in a temporally static (monofractal) manner across the entire run, thus averaging over trials and inputs. However, such a static analysis is not ideally suited for continuous naturalistic inputs, which often amount to a multifractal process with ever-changing and thus time-dependent scale-free dynamics. To accurately capture such dynamics we need to assess a time-dependent spectral exponent, β(t), rather than a static or complete run averaged value of β (Feder, 1988; Mandelbrot, 1999; Mahmoodi et al., 2020; Mahmoodi et al., 2023; West et al., 2023). Given the multifractal nature of real and continuous naturalistic inputs (Sabanal and Nakagawa, 1996; Luque et al., 2015; Voss and Clarke, 1978; Hsü and Hsü, 1991; Su and Wu, 2007; Levitin et al., 2012; González-Espinoza et al., 2017; Field, 1987; Nyikos et al., 1994; Field and Graham, 2007; Forsythe et al., 2011; Cutting et al., 2010; Cutting et al., 2012; Cutting et al., 2018) this raises the question of whether the brain's scale-free dynamics in auditory and visual regions also exhibit a time-dependent spectral exponent in response to continuous sensory inputs.

As an initial step in this direction, we ask and investigate whether scale-free brain dynamics are relevant during the exposure to naturalistic inputs, which, as discussed above, are often scale-free themselves. An attempt to investigate this question leads us to the concept of shared brain dynamics across subjects during naturalistic inputs, such as when watching a movie while lying in the scanner. Shared dynamics are measurable using inter-subject correlation (ISC) (Hasson et al., 2004; Hasson et al., 2010; Finn et al. 2018; Sonkusare et al., 2019; Finn and Bandettini, 2021; Finn 2021; Nguyen et al. 2022; Kringelbach et al., 2023). As demonstrated by recent studies, a potential indirect marker for input processing during naturalistic inputs is the degree of shared brain activity across subjects, namely ISC (Song et al., 2021; Jangraw et al., 2023). ISC typically measures the pairwise Pearson or Spearman correlations of time-series data between all possible subject pairs and then computes the mean or median correlation per brain region (Hasson et al., 2004; Hasson et al., 2010; Kauppi et al., 2010; Chen et al., 2016). Traditionally, ISC is calculated over the entire time-series, which averages out the time-varying nature of ISC, which, in turn, is very likely based on the simultaneously changing dynamics of sensory inputs (Hasson et al., 2004; Hasson et al., 2010; Sonkusare et al., 2019; Finn and Bandettini, 2021; Kringelbach et al., 2023). As a side note, ISC has also been applied at the subject level by averaging the ISC between one subject and all others to uncover individual neuronal and behavioral correlations (Finn et al., 2018; Nguyen et al., 2022).

Building upon the time-dependent nature of the spectral exponent β(t) of naturalistic sensory inputs and its potential imprint on the brain's simultaneously varying β(t), a first question arises: how might a dynamic, time-dependent measurement of inter-subject correlation, ISC(t), correlate with the brain's time-dependent spectral exponent in visual and auditory regions during naturalistic inputs? A potentially positive and significant correlation between β(t)-ISC(t) would provide inital evidence that the time-varying structure of the brain's spectral exponent relates to the degree of shared brain activity during continuous sensory inputs. However, a potentially positive β(t)-ISC(t) correlation leaves open the question of why the brain's time-dependent spectral exponent should be correlated or even functionally associated with the degree of shared brain activity over time, as measured through ISC(t).

The further investigation of this latter question leads us to recent studies that also applied a dynamic or time-dependent ISC analysis. These studies additionally demonstrated that the level or degree of ISC (t) can correspond with the subjects' cognitive performance or trait features (Song et al., 2021; Jangraw et al. 2023;Finn et al., 2018; Nguyen et al., 2022). In more detail, studies formed two groups of subjects and revealed that different levels of ISC between the two subject groups can correspond with task performance during activities such as reading (see Figure 6 in Jangraw et al., 2023). Studies further showed that ISC positively correlates with changes in emotional engagement and attentional focus when listening to a narrative story or watching a TV show episode (Song et al., 2021). Moreover, ISC levels between the two formed subject groups also correspond to the subjects' reading skills, with higher ISC observed in the group with better reading skills (see Figure 6 in Wat et al). Paradigmatically, the fMRI study by Jangraw et al. (2023) sorted subjects into two groups based on their reading ability scores from behavioral tests. During scanning, subjects had to read and listen to stories. The authors then computed time-dependent ISC for each group and observed that the group with higher reading performance exhibited significantly higher ISC across several brain regions. One possible explanation by the authors was that subjects with lower reading performance showed more idiosyncratic responses during the tasks. Conversely, subjects with higher reading performance processed the input in a more input-driven or objective matter, thus leading to higher ISC. Such an interpretation is also empirically supported by another study that used ISC to investigate stimulus-induced correlations. This study demonstrated that intrinsic or idiosyncratic brain dynamics remain uncorrelated across subjects during naturalistic inputs, while a stronger imprint of stimulus dynamics or properties leads to an increase in shared brain activity (Simony et al., 2016). Taken together, these studies provide evidence that the formation of groups based on specific criteria can positively correspond with different levels of ISC(t) during naturalistic inputs, so that, paradigmatically, better task performance or more cognitive or emotional engagement leads to higher levels of ISC(t) (Jangraw et al. 2023; Song et al. 2021).

To assess the extent to which brain dynamics capture and process input dynamics, our fMRI study builds on the two-group approach (Simony et al., 2016; Song et al., 2021; Jangraw et al., 2023). However, instead of using behavioral data for grouping absent in the investigated dataset, we return to the brain's activity itself as a basis for the two group formation. It is the brain's intrinsic activity that contributes an active component for successful input processing, that is, the relative rest-to-stimulus change of neuronal dynamics carries a functional role: the brain's spontaneous activity or resting-state often interacts in a non-additive fashion with inputs and consequently influences stimulus-induced activity and conscious perception (Sadaghiani et al., 2009; He, 2013; Huang et al., 2017; Podvalny et al., 2019; Northoff et al., 2024). We aim to provide evidence that the relative Rest-to-Movie change in the brain's scale-free dynamics modulates the level of shared brain activity during naturalistic inputs. The stronger the imprint of input properties on brain activity, the more the intrinsic or idiosyncratic components of brain dynamics are reduced. This leads to an increase in shared brain activity or ISC (Simony et al., 2016). Consequently, ISC can serve as an indirect marker for the alignment between the brain's activity and the input it receives.

Note that "alignment" is an umbrella term, similar to "adaptation" (Klar et al., 2023a; Klar et al., 2023b; for a review, see Northoff et al., 2023). In the context of our study, previous uses of the term focused on the intrinsic (rest) to stimulus changes in neuronal dynamics, particularly when these changes play a functional role in input processing (Huang et al., 2017; Klar et al., 2023a; Klar et al., 2023b; Northoff et al., 2023; Northoff et al., 2024). Our usage of the term "alignment" emphasizes the active component of the brain's spontaneous activity and its rest-to-stimulus changes, which can significantly influence stimulus-induced activity (Sadaghiani et al., 2009; He, 2013; Huang et al., 2017; Podvalny et al., 2019; Northoff et al., 2024). In the context of our study, alignment refers to the modulation and successful processing of naturalistic inputs by the brain's scale-free dynamics, indirectly assessed through ISC(t), along with their corresponding rest-to-movie changes.

To achieve the aforementioned aim of providing evidence that the relative Rest-to-Movie change of the brain's scale-free dynamics modulates the level of ISC, we apply a sliding window analysis (Tagliazucchi et al., 2016; Laumann et al., 2017; Huang et al., 2018; Jangraw et al. 2023) to reveal a time-dependent or dynamic spectral exponent β(t) and ISC(t) during movie-watching compared to the resting-state using the Human Connectome Project's 7 Tesla dataset (https://www.humanconnectome.org/). We investigate five cortical systems: the early visual, visual ventral stream, early auditory, auditory association, and dorsolateral prefrontal cortex (DLPFC) regions of the HCP MMP 1.0 atlas (Glasser et al., 2016). Our fMRI study includes four specific aims.

Aim one: We start our study by analyzing whether the brain's activity exhibits varying or time-dependent scale-free dynamics (β(t)) in response to the often encountered multifractal nature of naturalistic auditory and visual inputs (Feder, 1988; Mandelbrot, 1999; Mahmoodi et al., 2020; Mahmoodi et al., 2023; West et al., 2023). We hypothesize that the standard deviation (SD) of β(t) will be significantly higher during the movie run in visual and auditory regions compared to the resting-state. In contrast, the resting-state β(t) should remain relatively stable across regions due to the lack of varying input dynamics, reflected in a lower SD of β(t) during rest. We additionally analyze the DLPFC regions as control regions. We hypothesize that DLPFC regions lack significant β(t) changes between the movie and resting-state runs, due to their high anatomical and functional distance from early sensory input regions (Glasser et al., 2016; Rolls et al., 2022; Rolls et al., 2023a; Rolls et al., 2023b). In addition to β(t), we analyze ISC(t). We expect ISC(t) to fluctuate close to zero during the resting-state, but to significantly increase during shared inputs in the movie run in the visual and auditory regions.

Aim two: We expand on our analysis by applying ISC(t) alongside β(t) to demonstrate that the two measurements are positively correlated in visual and auditory regions during naturalistic inputs. Our hypothesis predicting a positive correlation between β(t) and ISC(t) in early input regions is based on the following reasoning: naturalistic auditory and visual stimuli comprise complex spatiotemporal patterns or dynamics that the brain must track to encode or process the input (for reviews on such brain-input coupling or matching, see Lakatos et al. 2019; Northoff et al. 2023; Northoff et al. 2024). Supporting this idea, a recent study by Campbell et al. (2022), which analyzed the same HCP 7 Tesla rest and movie dataset, found a significantly higher spectral exponent across regions of the cerebral cortex during the movie run compared to the resting-state. The continuous nature of naturalistic inputs requires the brain to adjust its dynamics to slower frequencies, which facilitates the temporal integration of many inputs. This is in contrast to the temporal segregation typically required in traditional and more discontinuous event-related paradigms (Honey et al., 2012; Hasson et al., 2015; Borges et al., 2018; Wolff et al., 2022; Northoff et al., 2023). If the dynamics of the input more effectively imprint themselves onto brain activity the brain's response becomes more stimulus-driven rather than being shaped by its intrinsic dynamics (Simony et al., 2016). In this case, we expect higher degrees of shared brain activity across subjects, as driven by the dynamics of external inputs and subsequently measured via a higher mean of ISC(t).

Aim three: Building on the analyses of aims one and two, we now investigate if and to what extent the brain's relative shift from intrinsic to stimulus-induced scale-free dynamics modulates the degree of shared brain activity during naturalistic inputs. To achieve this aim, we utilize ISC(t) by grouping subjects into two groups (Song et al., 2021; Jangraw et al., 2023) as follows: First, we group subjects into two groups for each brain region based on the subject-based Rest-to-Movie change in the standard deviation (SD) of the time-dependent spectral exponent β(t). Subjects with a decrease in Rest-to-Movie SD of β(t) are grouped in group one, while those with an increase are grouped in group two. We apply a region-based approach and grouping since we aim to understand how regional dynamics contribute to the level of ISC rather than focusing on subject-based data. Second, we compute ISC(t) during the movie run for the subjects in groups one and two. We hypothesize that the groups yield a significantly different mean of ISC(t) in visual and auditory regions modulated by the groups' individual Rest-to-Movie SD change in scale-free dynamics.

Aim four: In addition to demonstrating that the group with either an increase or decrease in the Rest-to-Movie SD change in β(t) yields a higher mean of ISC(t) during the movie run (aim three), we further aim to show that the group with the higher mean of ISC(t) also exhibits a stronger positive correlation of β(t) with ISC(t) in the visual and auditory regions during naturalistic inputs. A higher mean of ISC(t) together with a stronger β(t)-ISC(t) correlation within the same group would further support that the brain's Rest-to-Movie SD change in scale-free dynamics modulates the impact of input dynamics on the brain revealed by higher degrees of shared brain activity in one subject group compared to the other group. Thus, we hypothesize that the group with the higher mean of ISC(t) (as observed in aim three) also yields a higher positive β(t)-ISC(t) correlation. Conversely, we predict that the group with a lower mean of ISC(t) (as observed in aim three) shows a lower β(t)-ISC(t) correlation in the visual and auditory regions.

Finally, we replicated our analyses assessed in the MOVIE2 run by also investigating the MOVIE3 and MOVIE4 runs of the same HCP 7 Tesla dataset. Besides replicating our findings, these two additional movie runs also serve the purpose of probing for the movie-specificity of the time-dependent spectral exponent β(t) and ISC(t): we expect a different temporal structure of β(t) and ISC(t) in the three movie runs since each movie presented individual clips (with different audiovisual dynamics) to the same subjects. The analysis of the MOVIE3 and MOVIE4 runs beside MOVIE2 thus further allows us to tighten the relationship between β(t) and ISC(t) by demonstrating that the temporal structures of both measurements relate to specific temporal structures of the input (movie) dynamics. In short, these analyses further support the presumed close relationship between input and brain dynamics. Fig. 1 provides an overview of our study.

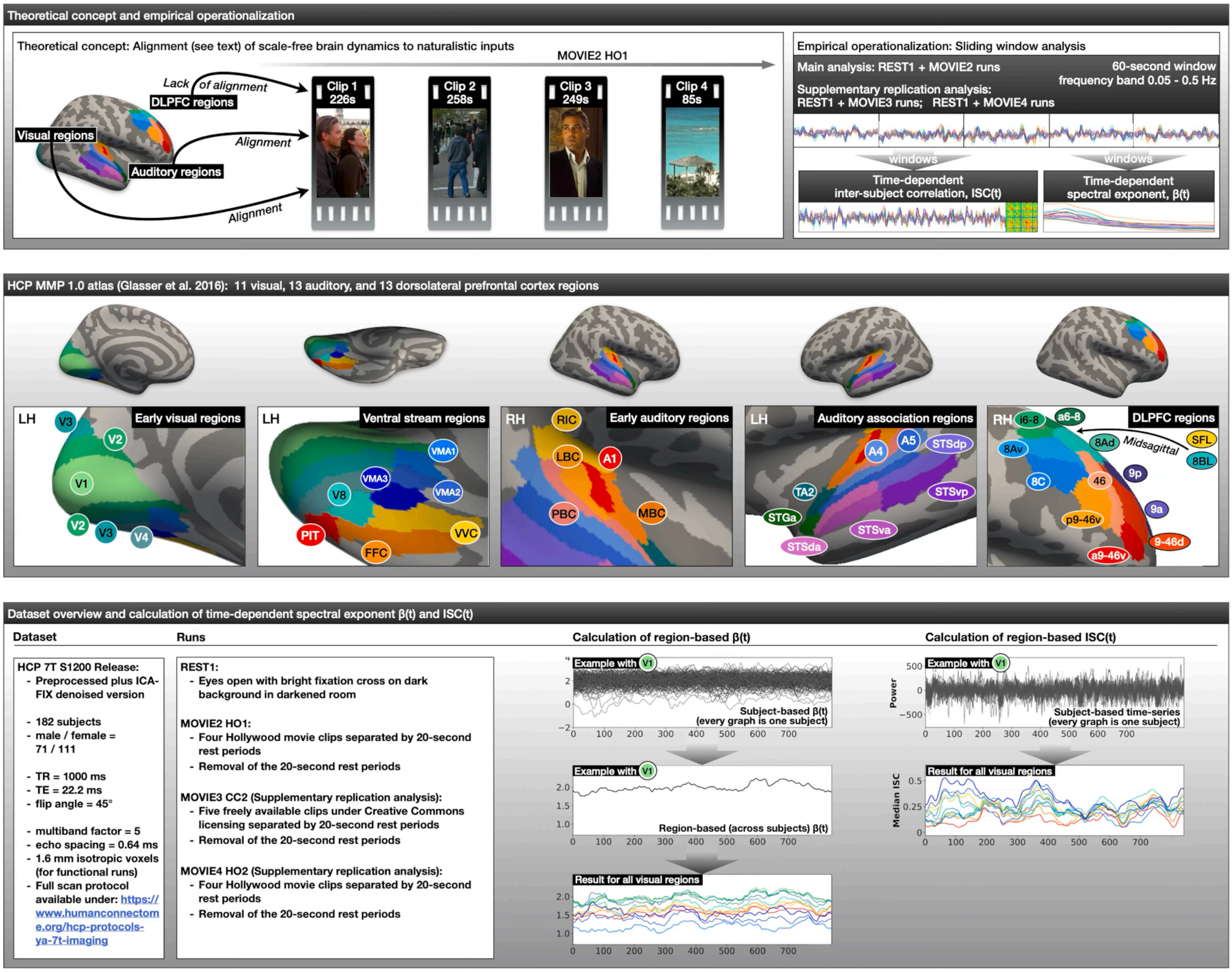

HCP 7T S1200 Release:
- Preprocessed plus ICA-FIX denoised version

- 182 subjects
- male / female = 71 / 111

- TR = 1000 ms
- TE = 22.2 ms
- flip angle = 45°

- multiband factor = 5
- echo spacing = 0.64 ms
- 1.6 mm isotropic voxels (for functional runs)
- Full scan protocol available under: https://www.humanconnectome.org/hcp-protocols-ya-7t-imaging

REST1:
- Eyes open with bright fixation cross on dark background in darkened room

MOVIE2 HO1:
- Four Hollywood movie clips separated by 20-second rest periods
- Removal of the 20-second rest periods

MOVIE3 CC2 (Supplementary replication analysis):
- Five freely available clips under Creative Commons licensing separated by 20-second rest periods
- Removal of the 20-second rest periods

MOVIE4 HO2 (Supplementary replication analysis):
- Four Hollywood movie clips separated by 20-second rest periods
- Removal of the 20-second rest periods

Fig. 1. Conceptual overview of our study and the HCP 7 Tesla resting-state and movie-watching dataset. Our main analysis investigated the REST1 and MOVIE2 runs. Our replication analyses used the HCP 7 Tesla REST1 versus MOVIE3 and REST1 versus MOVIE4 runs including the same subjects.

2. Methods

2.1. Subjects and study design

We included 182 subjects (male/female: 71/111; age span: 22-35 years) from the young adults Human Connectome Project (HCP, https://www.humanconnectome.org/) preprocessed plus ICA-FIX denoised 7 Tesla fMRI dataset. The scanning protocol, participant recruitment procedure, informed written consent forms, and consent to share deidentified data were approved by the Washington University institutional review board (van Essen et al., 2013). We investigated runs REST1 and MOVIE2 for our primary analysis. For supplementary analyses, we investigated REST1 with MOVIE3 and REST1 with MOVIE4. During the REST1 run, subjects had to keep their eyes open while fixating a projected bright cross-hair on a dark background presented in a darkened room. Subjects watched audiovisual Hollywood movie clips separated by 20-second rest periods in the MOVIE2 and MOVIE4 runs and freely available films under Creative Commons licensing in the MOVIE 3 run. The movie runs included a 20-second rest period before and after the final clip and between the single clips. We removed all 20-second rest periods from the three investigated movie runs.

2.2. Data acquisition

A Siemens MAGNETOM 7 Tesla MRI scanner housed at the Center for Magnetic Resonance (CMRR) at the University of Minnesota in Minneapolis acquired whole-brain scans. Physiological (cardiac and respiratory) recordings were not acquired. The scanner acquired gradient-echo echo-planar imaging (EPI) recordings with the following imaging parameters: time repetition = 1000 ms, time echo = 22.2 ms, flip angle = 45°, slice thickness = 1.6 mm (85 slices, 1.6 mm isotropic voxels for functional runs), field of view = 208 × 208 mm (RO x PE), matrix = 130 × 130 (RO x PE), multiband factor = 5, echo spacing = 0.64 ms, image acceleration factor = 2, partial Fourier sampling = 7/8, BW = 1924 Hz/Px. The complete scanning protocol is available at https://www.humanconnectome.org/hcp-protocols-ya-7t-imaging.

2.3. Preprocessing

We analyzed the so-called minimally preprocessed (Glasser et al., 2013) and ICA-FIX denoised (Salimi-Khorshidi et al., 2014; Griffanti et al., 2014) 7 Tesla dataset in standard volume NIfTI space without applying further preprocessing steps. A comprehensive preprocessing description is available in Glasser et al. (2013). Briefly, the preprocessing and ICA-FIX denoising included the following steps: (1) removal of spatial artifacts and distortions such as correction of MR gradient-nonlinearity-induced distortions for the anatomical scans; (2) nonlinear spatial normalization of the anatomical scans to MNI152 space and subsequent nonlinear functional to anatomical alignment (normalization) with a single spline interpolation that minimizes interpolation-induced blurring; (3) realignment of functional scans to compensate for subject head motion with a 6 DOF FLIRT registration of each frame to the single-bad reference image; (4) reduction of bias field; (5) normalization of the functional scans to a global mean and masking of the data with a final brain mask; and (6) cleaning of structured noise (denoising) via a pair of independent component analyses (MELODIC) with the FSL tool FIX to remove artefact components. The combination of ICA with the automated component classifier FIX was specifically trained on the HCP data. The HCP preprocessing pipeline excluded spatial smoothing, temporal filtering, slice timing correction, and motion censoring.

2.4. Time-dependent spectral exponent $\beta(t)$ analysis

We applied a sliding window approach previously applied in fMRI studies (Tagliazucchi et al., 2016; Laumann et al., 2017; Huang et al., 2018; Jangraw et al. 2023). Previous fMRI studies adopted various window lengths, spanning from seconds to minutes (Tagliazucchi et al., 2016; Laumann et al., 2017; Huang et al., 2018; Jangraw et al. 2023). Generally, shorter window lengths allow for capturing short-scaled changes in brain activity, while longer window lengths capture dynamics that are more stretched across time and comprise less variability, consequently capturing relatively longer-lasting changes. Contrary to fMRI sliding window studies with sometimes arbitrary window lengths, our chosen 60-second window with a one-second step increase equal to one fMRI time repetition rests on rational grounds: First, we avoided choosing very short windows, such as 20- or 30-second windows' to preserve a significant number of sampling points for β(t) and ISC(t) computation. Second, we individually adjusted the frequency band to 0.05-0.5 Hz so that the lowest frequency includes three complete cycles of the wavelength, increasing the precision of the power estimation in the Fourier transform required for the spectral exponent computation. Moreover, fMRI studies showed that frequencies beyond the often-chosen 0.1 Hz upper-frequency limit can include meaningful information not necessarily corrupted by noise (Shirer et al., 2015; Caballero-Gaudes and Reynolds, 2017). We decided to expand the upper frequency limit to 0.5 Hz, reflecting the Nyquist frequency due to the sampling rate of 1 Hz (TR = 1 s) in the 7 Tesla HCP dataset. A logarithmic transformation of fMRI power spectra (log-frequency and log-power) can follow a power-law distribution of $P = \frac{1}{f^{\beta}}$ where f is the frequency, P is the power, and the β is the spectral exponent. For every window we computed the β as follows: first, we transformed the BOLD signal of the time-domain into the frequency-domain via a discrete Fourier Transform (DFT) without applying a window function, smoothing, or tapering the data. We subsequently cut the power spectrum to the 0.05-0.5 Hz frequency band instead of band-passing the BOLD signal in the time-domain. The advantage of cutting the frequency band in the frequency-domain is that the power spectrum's power-law distribution remains preserved. Conversely, band-passing in the time-domain induces a roll-off near the lower and upper-frequency limit, diminishing the power spectrum's scale-free distribution. We finally applied the logarithm on the x-axis (frequency) and y-axis (power) and measured the spectral slope of the power distribution via a robust linear regression using repeated medians introduced by Siegel (1982) between log-frequency and log-power.

2.5. Time-dependent inter-subject correlation ISC(t) analysis

Hasson et al. (2004) introduced inter-subject correlation (ISC) analysis in fMRI. ISC can be implemented as a model-free approach for computing shared temporal patterns of brain activity between subjects, often measured during the presentation of naturalistic audiovisual inputs, such as during movie-watching or listening to music and speech (Hasson et al., 2004; Hasson et al., 2010; Hasson et al., 2015). Our fMRI analysis investigated a time-dependent ISC(t) via the same sliding window approach applied for the time-dependent spectral exponent β(t) analysis (60-second window with a one-second step increase). We computed ISC(t) as follows: first, we calculated each subject's mean time-series by averaging the time-series across all voxels per region. Next, we applied a fourth-order forward-backward (effectively an eight-order) Chebyshev Type I bandpass filter with the same frequency band of 0.05-0.5 Hz following our β(t) analysis on each subject's time-series. We subsequently computed the pairwise Pearson correlation coefficient between subjects for every window. Finally, we calculated the median Pearson correlation across subjects as a centrality statistic based on correlation coefficients of the lower triangle of the correlation matrix (excluding the diagonal line and upper triangle) for every window per region. Especially when using the pairwise correlation approach to compute ISC, the median can provide a more accurate summary of the Pearson correlation values across subjects than the mean (Chen et al., 2016). Choosing the median ISC instead across subjects also makes converting the r-values using the Fisher Z transform before taking the mean and converting the mean back to an r-value unnecessary, hence overcoming the back-and-forth transformation (Chen et al., 2016).

2.6. Regions of interest (ROIs)

We assessed (1) visual, (2) auditory, and (3) dorsolateral prefrontal cortex (DLPFC) regions of the HCP MMP 1.0 atlas (Glasser et al., 2016). The rationale behind the visual and auditory regions rests on the continuous audiovisual inputs from the movie clips. The DLPFC regions serve as control regions.

(1) Visual regions (11 regions): The visual regions include the early visual cortex and the ventral stream that spans from the visual cortex into the temporal lobe. The decision for the ventral stream (known as the "what pathway") instead of analyzing the dorsal stream extending into the parietal lobe (known as the "where pathway") rests on the well-established evidence that the ventral stream subserves visual object identification and recognition (Kriegeskorte et al., 2008; Bell et al., 2008), better matching the HCP movie-watching runs, whereas the dorsal stream primarily processes information about the position of objects relative to one's position in space It nonetheless requires consideration that the dorsal stream can also process simβ visual features (Pelekanos et al., 2016). Two fully independent visual streams might thus be a non-warranted simplification since the two streams include reciprocal interactions (Pelekanos et al., 2016). The early visual cortex comprises regions V1, V2, V3, and V4. The ventral stream comprises V8, ventral visual comβx (VVC), PIT comβx, fusiform face comβx (FFC), and three ventro-medial visual areas (VMA1, VMA2, and VMA3).
(2) Auditory regions (13 regions): The auditory regions include the early auditory A1, lateral belt comβx (LBC), medial belt comβx (MBC), para belt comβx (PBC), and retro-insular cortex (RIC). The auditory association cortex includes regions A4, A5, TCVp, STCVa, STSvp, STSva, STGa, and TA2. The auditory regions comβment the visual regions based on the audiovisual nature of the presented movie.
(3) DLPFC regions (13 regions): The DLPFC regions include areas 8C, 8Av, i6-8, s6-8, SFL, 8BL, 9p, 9a, 8Ad, p9-46v, a9-46v, 46, and 9-46d.

In addition to the HCP MMP 1.0 atlas publication (Glasser et al., 2016), a comprehensive anatomical and functional overview of the visual, auditory, and DLPFC regions is provided in the "Supplementary Neuroanatomical Results For A Multi-modal Parcellation of Human Cerebral Cortex" file available at https://www.nature.com/articles/nature18933. The HCP MMP 1.0 atlas used multi-modal magnetic resonance images from the Human Connectome Project and defined 180 areas per hemisphere based on cortical architecture, function, connectivity, and topography in a group average of 210 healthy young adults.

2.7. *Formation of two subject groups per region*

We applied a two-region group approach to use ISC(t) as adopted by previous studies (Song et al., 2021; Jangraw et al., 2023). Instead of grouping subjects based on behavioral data, we form two groups based on the brain's relative Rest-to-Movie change in scale-free dynamics since the brain's spontaneous activity often interacts in a non-additive fashion with inputs and consequently influences stimulus-induced activity and conscious perception (Sadaghiani et al., 2009; He, 2013; Huang et al., 2017; Podvalny et al., 2019; Northoff et al., 2024). We computed the Rest-to-Movie SD change of the time-dependent spectral exponent β(t) on a subject-based level individually for each region as follows: first, we computed the SD of β(t) in resting-state and movie runs per subject and region. In the second step, we formed two groups. Subjects with a Rest-to-Movie SD decrease of β(t) are grouped into group one per region, while we assign subjects with an increase to group two per region. This two-group approach allowed us to individually compute the region-based β(t) and ISC(t) in the movie run for groups one and two.

2.8. *Statistics and reproducibility*

We used the Bonferroni-Holm correction, also known as Holm's method (Holm, 1979), that controls the family-wise error rate (FWER) to counterbalance the problem of multiple comparisons (Neyman, 1937) due to repeating tests in statistical analyses. The reported *p*-values in our study are thus always Bonferroni-Holm adjusted *p*-values and use the following asterisk notation: $p < 0.05$*, $p < 0.01$**, and $p < 0.001$***. The advantage of the Bonferroni-Holm correction over the standard Bonferroni correction is that the former is less conservative and more powerful (Holm, 1979). The Bonferroni-Holm correction decreases the likelihood of type II (false negative) errors, meaning that potentially meaningful differences are deemed non-significant compared to the standard Bonferroni method. Briefly, after defining the significance threshold alpha (α), where we set $\alpha = 0.05$ in our analysis, the Bonferroni-Holm correction for multiβ comparisons functions as follows: (1) all obtained *p*-values are rank-ordered by their size, beginning with the smallest to the biggest *p*-value, with *m* being the number of *p*-values; (2) if the first *p*-value in the list of sorted *p*-values is greater than or equal to α/m, no *p*-values are significant; (3) after the first *p*-value potentially gains significance, the second *p*-value is then compared to α/m. If the second *p*-value is greater than or equal to $\alpha/(m\text{-}1)$, the remaining *p*-values are not significant. Otherwise, the procedure is repeated for the remaining *p*-values. We applied the Bonferroni-Holm correction individually for each analysis or family of tests. Specifically, we repeated the p-value correction for each analysis across the three modalities (visual, auditory, and DLPFC regions). For example, when we conducted three tests comparing the rest versus movie mean of ISC, we accordingly obtained three p-values which we corrected using the Bonferroni-Holm method.

2.9. *Supplementary replication analyses*

We conducted two complete and successful replication analyses where we investigated the REST1 and MOVIE3 and the REST1 and MOVIE4 runs instead of the REST1 and MOVIE2 runs (as for our primary analysis). In detail, our replication analyses include:

(1) Rest vs. movie differences in β(t): We investigated the mean and SD in the movie compared to the resting-state run in the REST1 versus MOVIE3 (Supplementary Figure 3a) and REST1 versus MOVIE4 (Supplementary Figure 3b) runs. Noteworthy, a visual inspection and comparison shows that β(t) showed a different temporal structure between all three movie runs, providing further evidence that the time-dependent β(t) is a potential response to each movie's individual ever-changing input β(t).

(2) Rest vs. movie differences in ISC(t): We investigated the mean of ISC(t) in the movie compared to the resting-state run in the REST1 versus MOVIE3 (Supplementary Figure 4a) and REST1 versus MOVIE4 (Supplementary Figure 4b) runs. As observed for β(t), a visual inspection and comparison between the three assessed movie runs shows that ISC(t) yielded a different temporal structure between all three movie runs.

(3) Spearman correlation between β(t) and ISC(t) in the movie run for all subjects: We investigated the β(t)-ISC correlations in MOVIE3 (Supplementary Figure 5a) and in MOVIE4 (Supplementary Figure 5b).

(4) ISC(t) for groups 1 and 2 in the movie run: We investigated the mean of ISC(t) in Group 1 compared to Group 2 in MOVIE3 (Supplementary Figure 6a) and in MOVIE4 (Supplementary Figure 6b).

(5) Spearman correlation between β(t) and ISC(t) for groups 1 and 2 in the movie run: We investigated the β(t)-ISC correlation in Group 1 compared to Group 2 in MOVIE3 (Supplementary Figure 7a) and MOVIE4 (Supplementary Figure 7b).

(6) Scale-free dynamics based on the Supplementary resting-state and movie runs: We also checked that the complete (instead of sliding window-based) runs exhibit scale-free dynamics. We computed the power spectrum in the same frequency band (0.05-0.5 Hz) as for our sliding window analysis but based on the complete runs. Supplementary Figure 9 shows the complete run power spectra for the visual, auditory, and DLPFC regions.

3. Results

3.1. *Higher Mean and SD of the time-dependent spectral exponent β(t) during naturalistic inputs compared to the resting-state*

For aim one, we hypothesized that the brain's scale-free dynamics exhibit a time-dependent spectral exponent β(t) in auditory and visual regions during naturalistic inputs. We measured a significantly higher mean and standard deviation (SD) of β(t) in the movie run in visual and auditory regions compared to the resting-state. Note that the p-values of all our analyses underwent Bonferroni-Holm correction (see method section for details).

Mean results: We observed a significantly higher mean of β(t) in the movie run compared to the resting-state in visual ($t = -4.5$, $p = 0.001$) and auditory ($t = -7.47$, $p < 0.001$) regions. The DLPFC regions lacked a significant rest versus movie mean difference ($t = -0.02$, $p = 0.987$).
SD results: We also observed a significantly higher SD of β(t) in the movie run compared to the resting-state in visual ($t = -11.58$, $p < 0.001$), auditory ($t = -12.9$, $p < 0.001$) and DLPFC regions ($t = -3.53$, $p = 0.004$). Fig. 2a displays β(t) in the resting-state and the movie run, while Fig. 2b shows the statistical results.

We replicated the significantly higher mean and SD of β(t) in the movie run compared to the resting-state in the REST1 versus MOVIE3 comparison (Supplementary Figure 1a) and in the REST1 versus MOVIE4 comparison (Supplementary Figure 1b). A visual inspection of β(t) in Figure 2a reveals that β(t) remains relatively stable during the resting-state. In contrast, during the movie runs, β(t) exhibits a distinct temporal structure that varies between the visual and auditory regions. Furthermore, β(t) in the visual and auditory regions differs substantially across all three movie runs (MOVIE2, MOVIE3, and MOVIE4). We propose that the distinct audiovisual inputs of the three movies require different responses in the brain's scale-free dynamics, as reflected in the varying β(t) profiles observed across the three movies. Finally and in yet another control analysis, we also investigated whether the complete

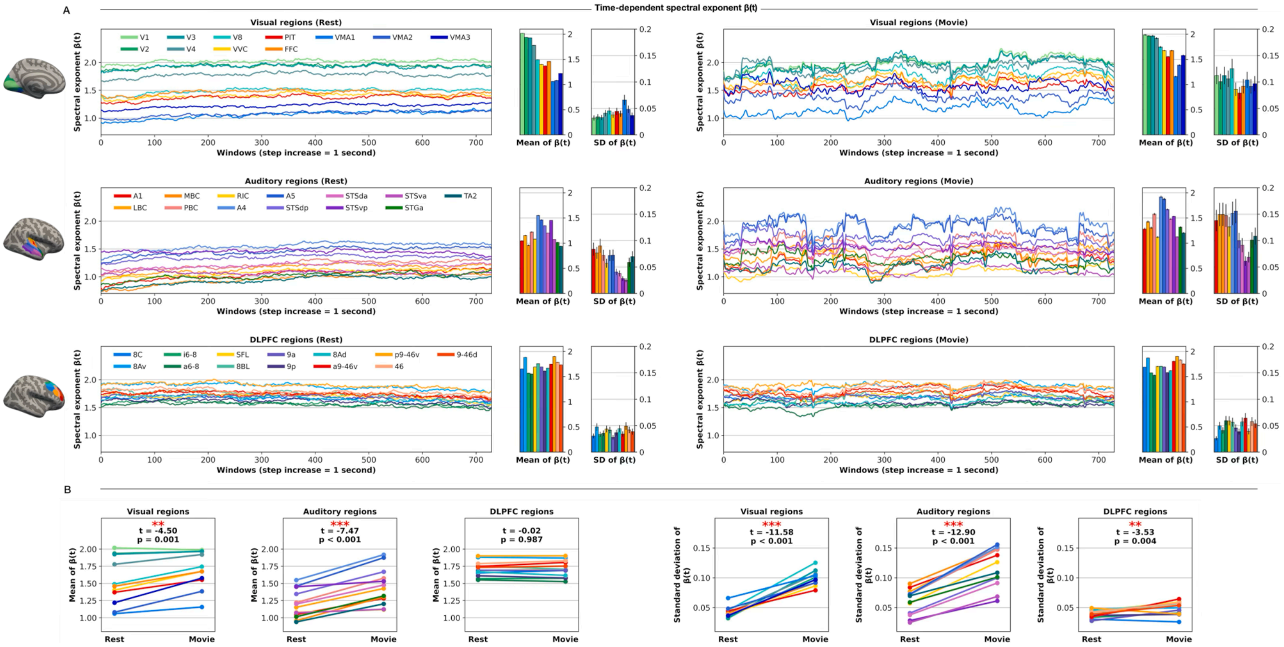

Fig. 2. Time-dependent spectral exponent β(t) in the REST1 and MOVIE2 runs. a) β(t) in visual, auditory, and DLPFC regions. b) Paired *t*-tests between REST1 and MOVIE2. (SD standard deviation, significance asterisks $p < 0.05$ *, $p < 0.01$ **, $p < 0.001$ ***, *p*-value correction = Bonferroni-Holm, error bars = 95% confidence interval).

resting-state and movie runs (rather than the sliding window-based analysis) exhibit power-law distributions. To do this, we computed the power spectrum over the same frequency band (0.05–0.5 Hz) used in our time-dependent or sliding window analysis. Supplementary Figure 9 displays the power spectra for the complete runs in the visual, auditory, and DLPFC regions in the rest and movie runs.

3.2. Higher mean of time-dependent ISC(t) during naturalistic inputs compared to the resting-state

Aim one also involved measuring the time-dependent ISC(t) during both the resting-state and the movie run. We hypothesized, and observed, that ISC(t) fluctuates around zero in the resting-state, while the mean of ISC(t) significantly increased during the movie run in the

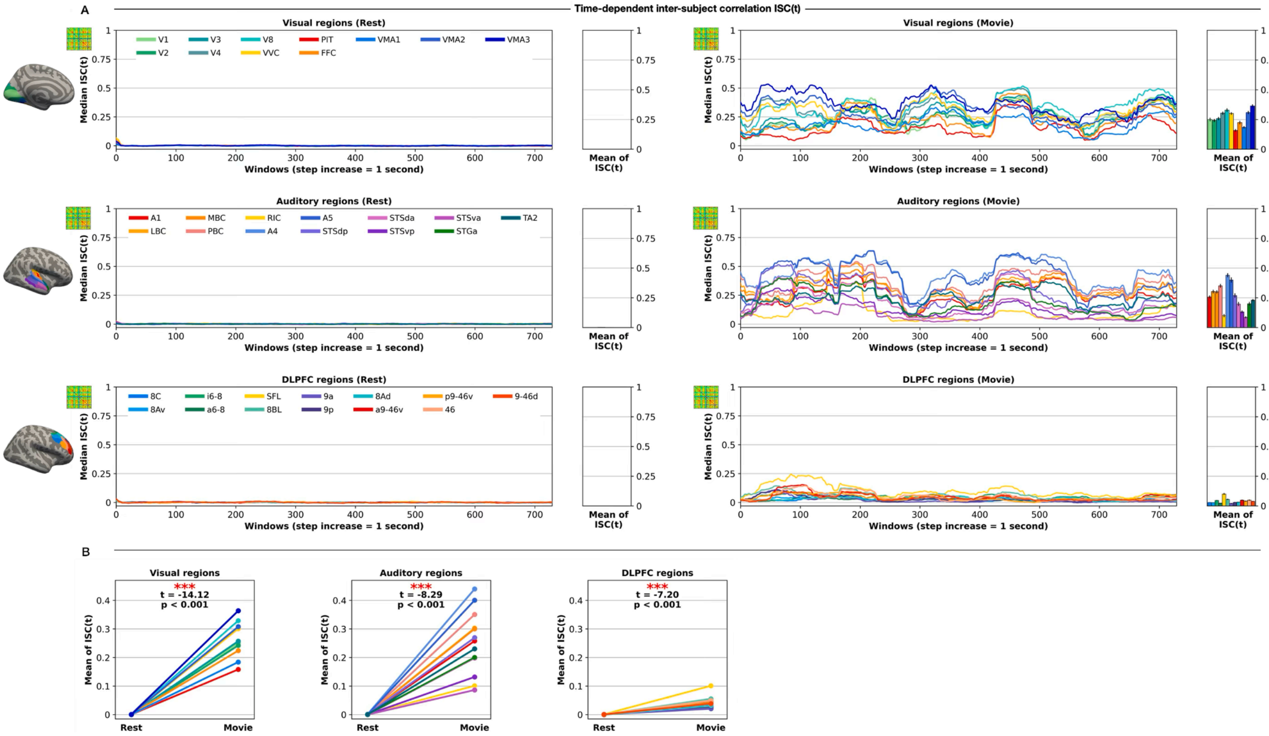

Fig. 3. Time-dependent ISC(t) in the REST1 and MOVIE2 runs. a) ISC(t) in visual, auditory, and DLPFC regions. b) Paired *t*-tests between REST1 and MOVIE2. (significance asterisks $p < 0.05$ *, $p < 0.01$ **, $p < 0.001$ ***, *p*-value correction = Bonferroni-Holm, error bars = 95% confidence interval).

visual ($t = -14.12$, $p < 0.001$), auditory ($t = -8.29$, $p < 0.001$), and DLPFC ($t = -7.2$, $p < 0.001$) regions. We replicated the significantly higher mean of ISC(t) in the movie run compared to the resting-state in the visual, auditory, and DLPFC regions in both the REST1 versus MOVIE3 comparison (Supplementary Figure 2a) and the REST1 versus MOVIE4 comparison (Supplementary Figure 2b). As observed for $\beta(t)$ in the visual and auditory regions in Fig. 2a, ISC(t) also exhibits a specific temporal structure that differs substantially across the three movie runs (MOVIE2, MOVIE3, and MOVIE4).

3.3. Correlation between β(t) and ISC(t) during naturalistic inputs

We observe a similar temporal structure between $\beta(t)$ and ISC(t) (Figs 2a and 3a) for the visual and auditory regions in the movie run. Interestingly, a similar temporal structure between $\beta(t)$ and ISC(t) can also be seen for the MOVIE3 and MOVIE4 runs (see Supplementary results). This observation leads us to our second aim, namely to demonstrate a positive correlation between $\beta(t)$ and ISC(t). We used Spearman's rank correlation to assess the relationship between $\beta(t)$ and ISC(t) for each region individually (Fig. 4).

Visual regions: We obtained significant and positive $\beta(t)$-ISC(t) correlations in all visual regions ($p < 0.001$ for every visual region). The average correlation across all visual regions is $\rho = 0.5$.

Auditory regions: We also observed significant and positive $\beta(t)$-ISC(t) correlations in all auditory regions ($p < 0.001$ for every auditory region). The average correlation across all auditory regions is $\rho = 0.72$.

DLPFC regions: The DLPFC regions showed a mix of positive and negative correlations, which were generally weaker than those observed in the visual and auditory regions. Given the mix of positive and negative correlations, the average correlation across all DLPFC regions was $\rho = -0.11$.

We replicated the positive $\beta(t)$-ISC(t) correlations in the MOVIE3 run (visual regions mean $\rho = 0.42$; auditory regions $\rho = 0.65$; DLPFC regions $\rho = -0.06$) as shown in Supplementary Figure 3a, and in the MOVIE4 run (visual regions mean $\rho = 0.55$; auditory regions $\rho = 0.63$; DLPFC regions $\rho = 0$) as shown in Supplementary Figure 3b. The moderate to strong $\beta(t)$-ISC(t) correlations in the visual and auditory regions suggest that the temporal structure or level of $\beta(t)$ systematically varies with the level of ISC(t), highlighting their functional connection: higher $\beta(t)$ levels are positively correlated with higher ISC(t) levels.

3.4. The rest-to-movie SD change in β(t) modulates the mean of ISC(t) during naturalistic inputs

So far, aim one demonstrated that the brain's scale-free dynamics exhibit a time-dependent spectral exponent $\beta(t)$ in the three assessed movie runs, especially in visual and auditory regions. In aim two we also demonstrated that $\beta(t)$ positively correlates highly with ISC(t) in visual and auditory regions. Our analyses rested on a region-based level. When zooming in and assessing the subject-based level $\beta(t)$, we observe a high variance between the single subjects' SD of $\beta(t)$ during naturalistic inputs, shown in Fig. 5 for the early visual and early auditors regions. (Note that Supplementary Figure 4 shows the subject-based $\beta(t)$ for the movie run in the ventral stream and auditory association regions, while Supplementary Figure 5 shows the same in the DLPFC regions.)

Previous studies have shown that the brain's intrinsic spontaneous activity often interacts non-additively with external inputs, meaning that neuronal activity during inputs can be significantly modulated by the change in brain activity from rest to stimulus states (Sadaghiani et al., 2009; He, 2013; Huang et al., 2017; Podvalny et al., 2019; Northoff et al., 2024). Building on the high variability in the time-dependent structure of $\beta(t)$ across subjects, we now assess how different degrees of Rest-to-Movie SD changes in scale-free dynamics impact the level or mean of ISC(t) during naturalistic inputs. To achieve this, we use the two-group approach described in the introduction and methods sections of our study (Song et al., 2021; Jangraw et al., 2023). Briefly, we created two groups for each region based on the subject-specific Rest-to-Movie SD change of $\beta(t)$. Subjects with a decrease in Rest-to-Movie SD of $\beta(t)$ are placed in Group 1, while those with an increase are assigned to Group 2 for each region. This approach allowed us to investigate whether Group 1, with a Rest-to-Movie SD decrease in $\beta(t)$, or Group 2, with an increase, shows a significantly higher mean of ISC(t) in the movie run. Fig. 6a presents the results for

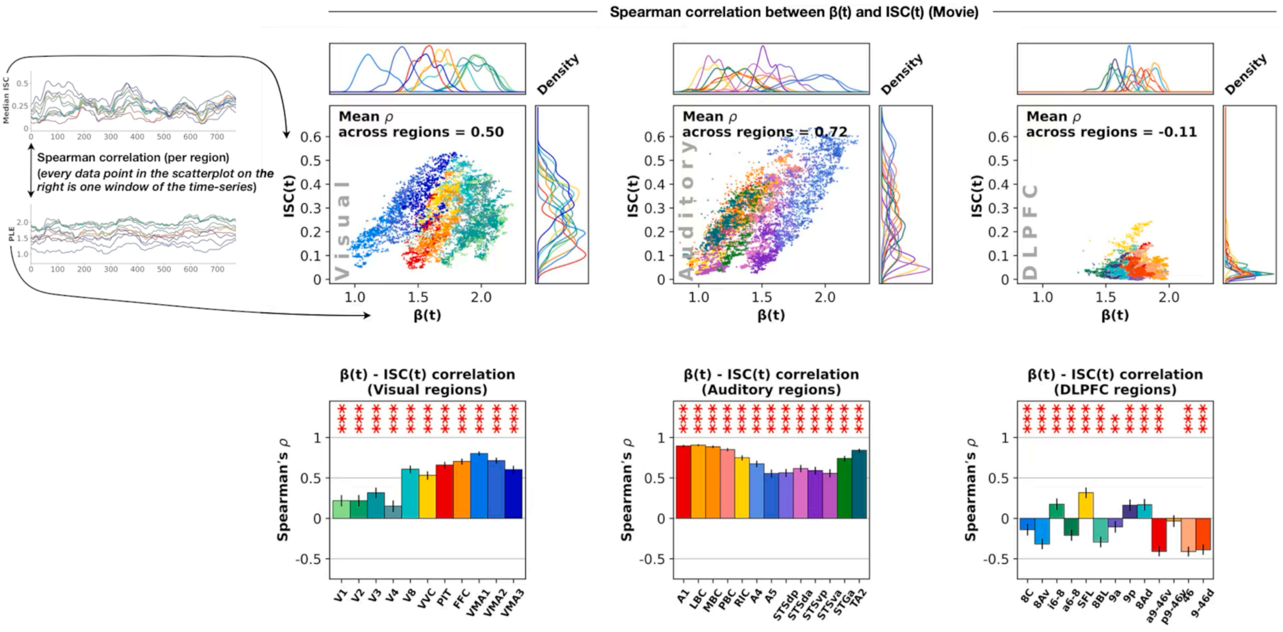

Fig. 4. Spearman's rank correlation between $\beta(t)$ and ISC(t) in the MOVIE2 run. We correlated the windows of $\beta(t)$ with the windows of ISC(t) in every region. Every data point in the scatterplots represents one window or data point of $\beta(t)$ and ISC(t). (significance asterisks $p < 0.05$ *, $p < 0.01$ **, $p < 0.001$ ***, p-value correction = Bonferroni-Holm, error bars = 95% confidence interval).

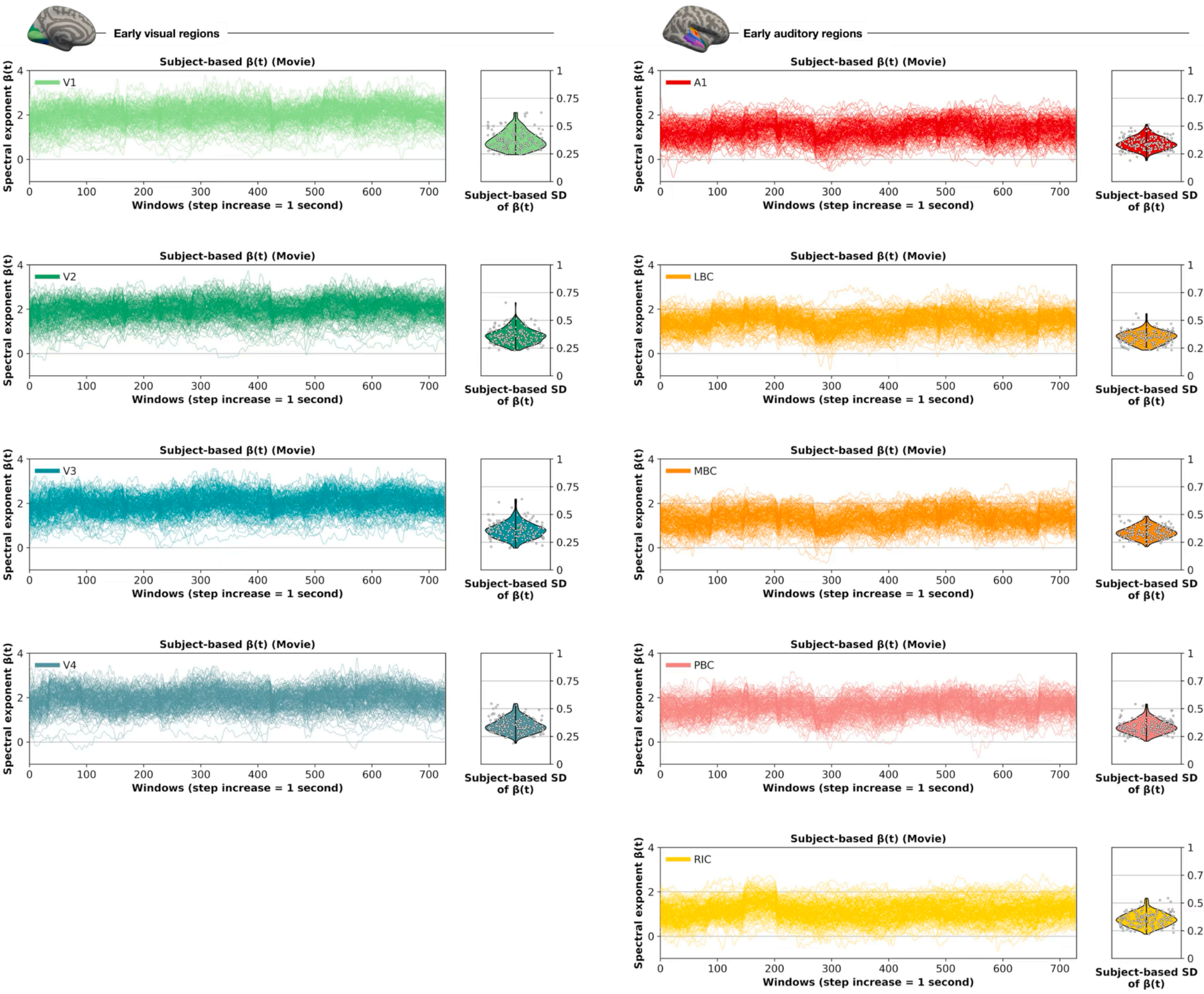

Fig. 5. Subject-based β(t) and its SD in the MOVIE2 run in early visual (left side) and early auditory (right side) regions. Every graph represents the β(t) of one subject per region. (SD standard deviation, $n = 182$ subjects).

the two groups, where each data point represents the Rest-to-Movie SD decrease or increase for each subject per region. Fig. 6b shows four paradigmatic subjects with a Rest-to-Movie SD decrease and four subjects with a Rest-to-Movie SD increase in visual region V1 and auditory region A1.

We analyzed ISC(t) individually for both groups, as shown in Fig. 7a, and statistically compared the mean ISC(t) between the groups, as shown in Fig. 7b.

> Visual regions: Group 1 yielded a higher mean of ISC(t) in the visual regions than Group 2 ($t = 5.8$, $p < 0.001$).
> Auditory regions: Group 1 also yielded a higher mean of ISC(t) in the auditory regions than group 2 ($t = 3.14$, $p = 0.002$).
> DLPFC regions: The DLPFC lacked a significant difference in the mean of ISC(t) between both groups ($t = 0.99$, $p = 0.33$).

We replicated the significantly higher mean of ISC(t) in Group 1 for the MOVIE3 run in both the visual ($t = 7.64$, $p < 0.001$) and auditory ($t = 3.52$, $p < 0.001$) regions, as shown in Supplementary Figure 4a, and for the MOVIE4 run in the visual ($t = 6.37$, $p < 0.001$) and auditory ($t = 2.58$, $p = 0.004$) regions, as shown in Supplementary Figure 4b. As previously observed in the analysis of all subjects, while ISC(t) was generally higher for Group 1 compared to Group 2, the temporal structure of ISC(t) differed between the three movie runs.

3.5. *Higher positive β(t)-ISC(t) correlation in Group 1 than in Group 2 during naturalistic inputs*

As previously investigated for all subjects in aim two, we repeated the β(t)-ISC(t) correlation analysis for the two groups. We hypothesized that Group 1, which showed a higher mean of ISC(t) in the visual and auditory regions during the movie run, would also exhibit a stronger positive correlation between the temporal structures of β(t) and ISC(t).

> Visual regions: We observed significant and positive β(t)-ISC(t) correlations in all visual regions ($p < 0.001$ for every visual region) for Group 1. The average correlation across all visual regions for Group 1 is $\rho = 0.59$. The average correlation across all visual regions for Group 2 is lower than in Group 1, $\rho = 0.40$. The statistical comparison between Group 1 and Group 2 in the visual regions yielded significantly higher β(t)-ISC(t) correlations for Group 1 ($t = 1.94$, $p = 0.034$).
> Auditory regions: We also observed significant and positive β(t)-ISC(t) correlations in all auditory regions ($p < 0.001$ for every visual region) for Group 1. The average correlation across all auditory regions for Group 1 is $\rho = 0.74$. The average correlation across all auditory regions for Group 2 is lower than in Group 1, $\rho = 0.65$. The statistical comparison between Group 1 and Group 2 in the auditory regions lacked a significant difference ($t = 1.44$, $p = 0.082$).
> DLPFC regions: The DLPFC regions in Group 1 yielded a mixture of positive and negative correlations that were generally weaker than in

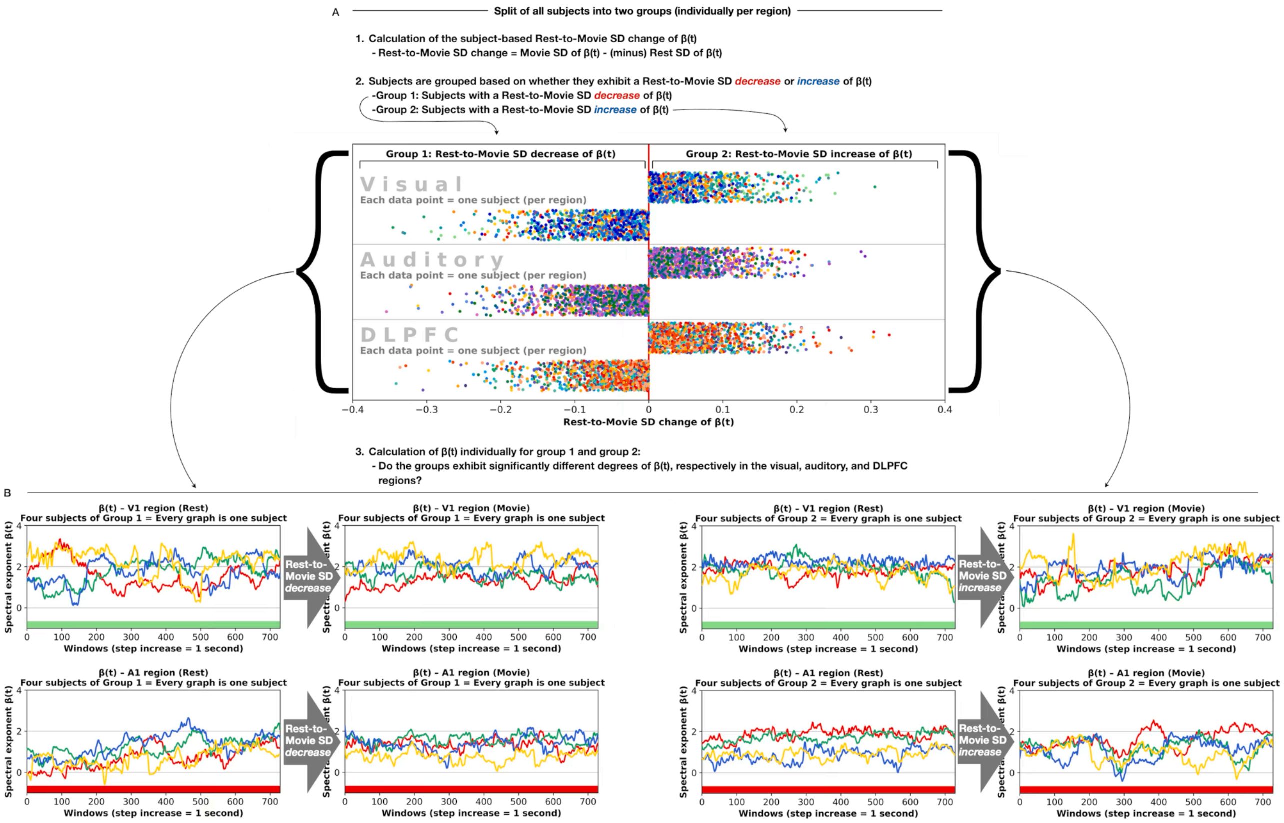

1. Calculation of the subject-based Rest-to-Movie SD change of β(t)
   - Rest-to-Movie SD change = Movie SD of β(t) - (minus) Rest SD of β(t)
2. Subjects are grouped based on whether they exhibit a Rest-to-Movie SD *decrease* or *increase* of β(t)
   - Group 1: Subjects with a Rest-to-Movie SD *decrease* of β(t)
   - Group 2: Subjects with a Rest-to-Movie SD *increase* of β(t)
3. Calculation of β(t) individually for group 1 and group 2:
   - Do the groups exhibit significantly different degrees of β(t), respectively in the visual, auditory, and DLPFC regions?

Fig. 6. The Figure illustrates the formation of two groups per region based on the subject-based Rest-to-Movie SD change in scale-free dynamics, enabling a subsequent group-based ISC(t) analysis. a) Subjects with a Rest-to-Movie SD decrease of β(t) are grouped into Group 1 (left side of the Figure), while we group subjects with an increase into Group 2 (right side of the Figure). Every data point reflects the Rest-to-Movie SD change of β(t) for each subject per region. b) Shown are four paradigmatic subjects with a Rest-to-Movie SD decrease (left side) and four subjects with a Rest-to-Movie SD increase (right side) in visual region V1 and auditory region A1.

the visual and auditory regions. Due to the weaker positive and negative correlations, the average correlation across all DLPFC regions in Group 1 amounts to zero ρ = -0.04. We observed a similar mixed pattern for Group 2 with an average correlation across all DLPFC regions of ρ = -0.16. The statistical comparison between Group 1 and Group 2 in the DLPFC regions lacked a significant difference ($t = 1.09$, $p = 0.288$). Fig. 8a displays the β(t)-ISC(t) correlation for Group 1, Fig. 8b for Group 2, and Fig. 8c shows the statistical comparisons between the two groups. We replicated the significantly higher β(t)-ISC(t) correlation in Group 1 compared to Group 2 in the MOVIE3 run in the visual regions ($t = 1.8$, $p = 0.045$) shown in Supplementary Figure 5. The MOVIE4 lacked significant differences in the visual, auditory, and DLPFC regions, as shown in Supplementary Figure 6.

Taken together with the previous two-group analysis during the movie run (Fig. 7), the β(t)-ISC(t) correlation demonstrates that that Group 1 (Rest-to-Movie SD decrease of β(t)) yielded both a significantly higher mean of ISC(t) in visual and auditory regions and a significantly higher β(t)-ISC(t) correlation in visual and auditory regions than Group 2 (Rest-to-Movie SD increase of β(t)).

4. Discussion

Our fMRI study represents an initial step in demonstrating that the brain's scale-free dynamics exhibit a time-dependent structure in response to continuous naturalistic auditory and visual inputs. The brain's dynamic rather than static spectral exponent β(t) demonstrated by our first aim is a likely response to the multifractal nature often encountered in real-world and naturalistic inputs (Feder, 1988; Mandelbrot, 1999; Mahmoodi et al., 2020; Mahmoodi et al., 2023; West et al., 2023). In contrast to the movie run, we observed a stable spectral exponent β(t) with only minor fluctuations and no distinct temporal structure in the resting-state, as subjects maintained a constant fixation on a bright crosshair against a dark background in a darkened room. The observed spectral stability suggests that, in the absence of dynamic auditory and visual inputs, the brain's scale-free dynamics do not require significant adjustments with inputs, resulting in a stable spectral exponent in the resting-state.

In contrast and during movie-watching, the brain's spectral exponent β(t) displayed a temporal structure that also diverged between visual and auditory regions, likely reflecting the ever-varying properties specific to auditory and visual inputs. Additionally, the temporal structure of scale-free dynamics in the visual and auditory regions differed across the three analyzed movie runs (see Supplementary Figures 1a and 1b), likely due to the audiovisual characteristics that are distinctive of each movie clip. More generally, we show that the spectral exponent of a biological system, such as the brain, aligns with the time-dependent or multifractal spectral exponents of incoming inputs; this notion is rooted in the complexity matching framework originating from the biological domain of fractal physiology (West et al., 2023; Mahmoodi et al., 2023; West, 2024).

For our second aim, we demonstrated that the time-dependent spectral exponent β(t) positively correlates with time-dependent intersubject correlation (ISC(t)) in both visual and auditory regions. How can we explain the positive β(t)-ISC(t) correlation, so that higher spectral exponents go along with higher degrees of shared brain activity in response to inputs? First, recall that in the analysis for aim one, we found a significant increase in the mean of the spectral exponent during the presentation of naturalistic inputs. This is a likely result due to the more

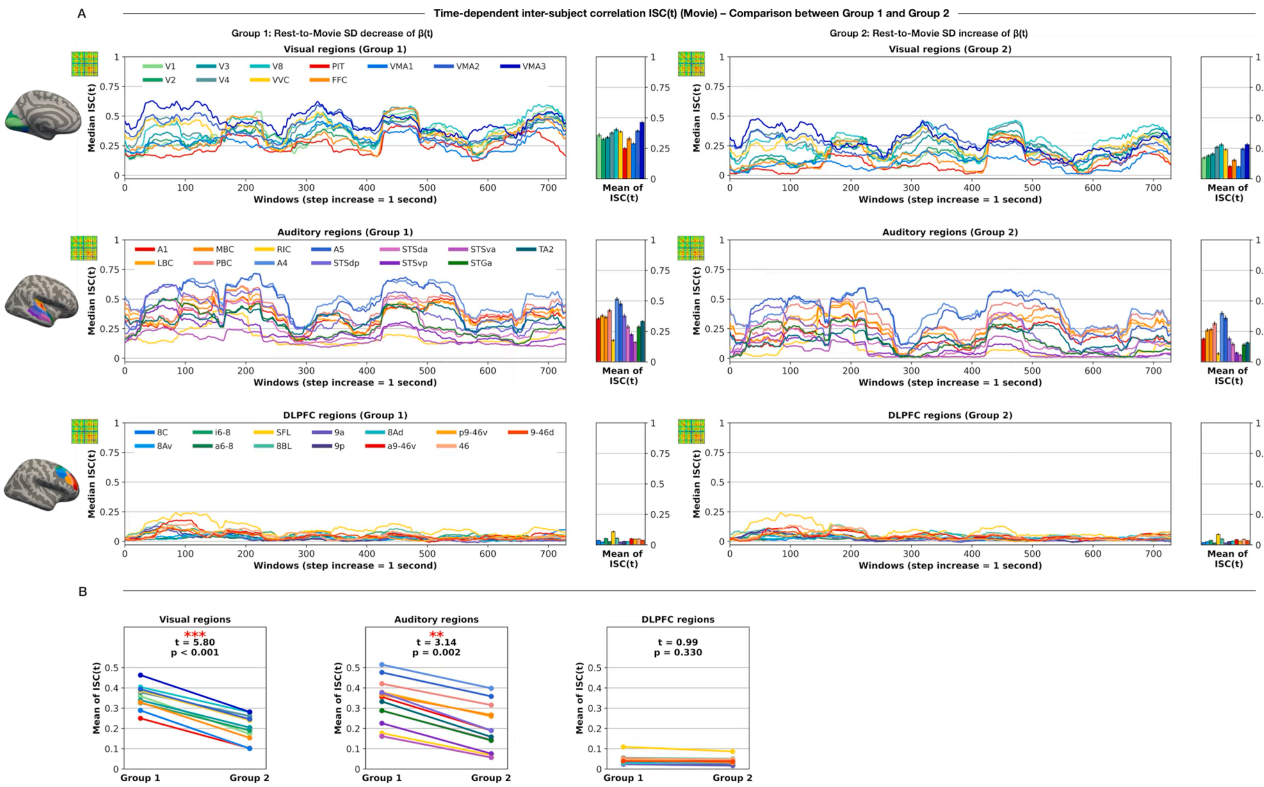

Fig. 7. Time-dependent ISC(t) during the MOVIE2 run in two groups. a) The left side of the plot shows Group 1 (based on the Rest-to-Movie SD decrease of β(t)) and the right side of the plot shows Group 2 (based on the Rest-to-Movie SD increase of β(t)). b) Independent *t*-tests between Group 1 and Group 2 in visual, auditory, and DLPFC regions. (Significance asterisks $p < 0.05$ *, $p < 0.01$ **, $p < 0.001$ ***, p-value correction = Bonferroni-Holm, error bars = 95% confidence interval).

complex and fractal nature of the audiovisual properties in the movie, compared to the eyes-open resting-state where subjects are exposed to monotonous scanner noise while visually fixating on the head coils and MRI scanner walls. As the movie's audiovisual input dynamics more strongly influence brain activity, the brain's response becomes increasingly stimulus-driven and less shaped by its intrinsic dynamics (Simony et al., 2016).

Additionally, the movie's continuous audiovisual inputs very likely possess a higher fractal or nested temporal structure than the brain's stimulus-free resting-state, forcing the brain's dynamics to elevate their spectral exponent over time, as per the complexity matching phenomenon (West et al., 2023; Mahmoodi et al., 2023; West, 2024). Studies of complexity matching demonstrated that a less complex system, such as the brain with a lower spectral exponent that we observed the resting-state, aligns with a more complex system, such as the movie's audiovisual inputs, by increasing its complexity, such as via the spectral exponent, as observed in the movie run (West et al., 2023; Mahmoodi et al., 2023; West, 2024). In conclusion, subjects who align their scale-free dynamics more closely with those of the input exhibit more similar brain activity during continuous naturalistic inputs, since an improved brain-input matching naturally results in a stronger footprint of the input on brain dynamics in early sensory regions leading to higher ISC.

Importantly, the positive correlation between β(t) and ISC(t) follows previous findings from an electrocorticographic study by Honey et al. (2012), where the authors observed that steeper power spectrum slopes or exponents were associated with higher degrees of shared brain activity or ISC during intact movie conditions, as opposed to scrambled movie conditions. Again, naturalistic ongoing inputs (Feder, 1988; Mandelbrot, 1999; Mahmoodi et al., 2020; Mahmoodi et al., 2023; West et al., 2023) and intact movies (Cutting et al., 2010; Cutting et al., 2012; Cutting et al., 2018) exhibit a time-dependent or multifractal spectral exponent due to their ever-changing contents, which is lost when inputs undergo scrambling or shuffling, then resulting in a stable or constant white noise process.

One might wonder why the β(t)-ISC(t) correlation is strongly positive rather than negative, and how the correlation might differ during non-continuous, event-related inputs. The positive β(t)-ISC(t) correlation can be explained by the fact that higher spectral exponents indicate a shift of power from faster to slower frequencies, which supports higher degrees of temporal integration necessary for processing continuous inputs, such as during movie-watching (Honey et al., 2012; Hasson et al., 2015; Borges et al., 2018; Wolff et al., 2022; Northoff et al., 2023). Recall from the introduction that higher spectral exponents correspond to longer temporal correlations, as indicated by higher values of the Hurst exponent in the time-domain (Mandelbrot, 1999; Linkenkaer-Hansen et al., 2001; Hardstone et al. 2012). One of our findings demonstrated a significantly higher mean of the time-dependent spectral exponent in sensory regions during inputs compared to the resting-state. This observation was also made in a recent fMRI study using the same HCP 7 Tesla dataset (Campbell et al., 2022): the authors found a significantly higher spectral exponent across multiple cortical regions during inputs than in the resting-state. Conversely, higher degrees of temporal segregation are required in fast event-related designs, where β can decrease (He, 2011; Kasagi et al., 2017; Wainio-Theberge et al., 2022).

Thus, higher spectral exponents likely allowed a better imprinting of audiovisual input properties on the brain's ongoing neuronal dynamics, as reflected by higher degrees of ISC including a positive β(t)-ISC(t) correlation. But what would the β(t)-ISC(t) correlation potentially look like if subjects underwent an event-related design, with temporally discontinuous or discrete inputs rather than continuous and contiguous inputs? In this case, neuronal dynamics would likely need to decrease their spectral exponent to optimize the processing of the temporally segregated inputs effectively, as previously shown by other studies (He, 2011; Kasagi et al., 2017; Wainio-Theberge et al., 2022), then likely

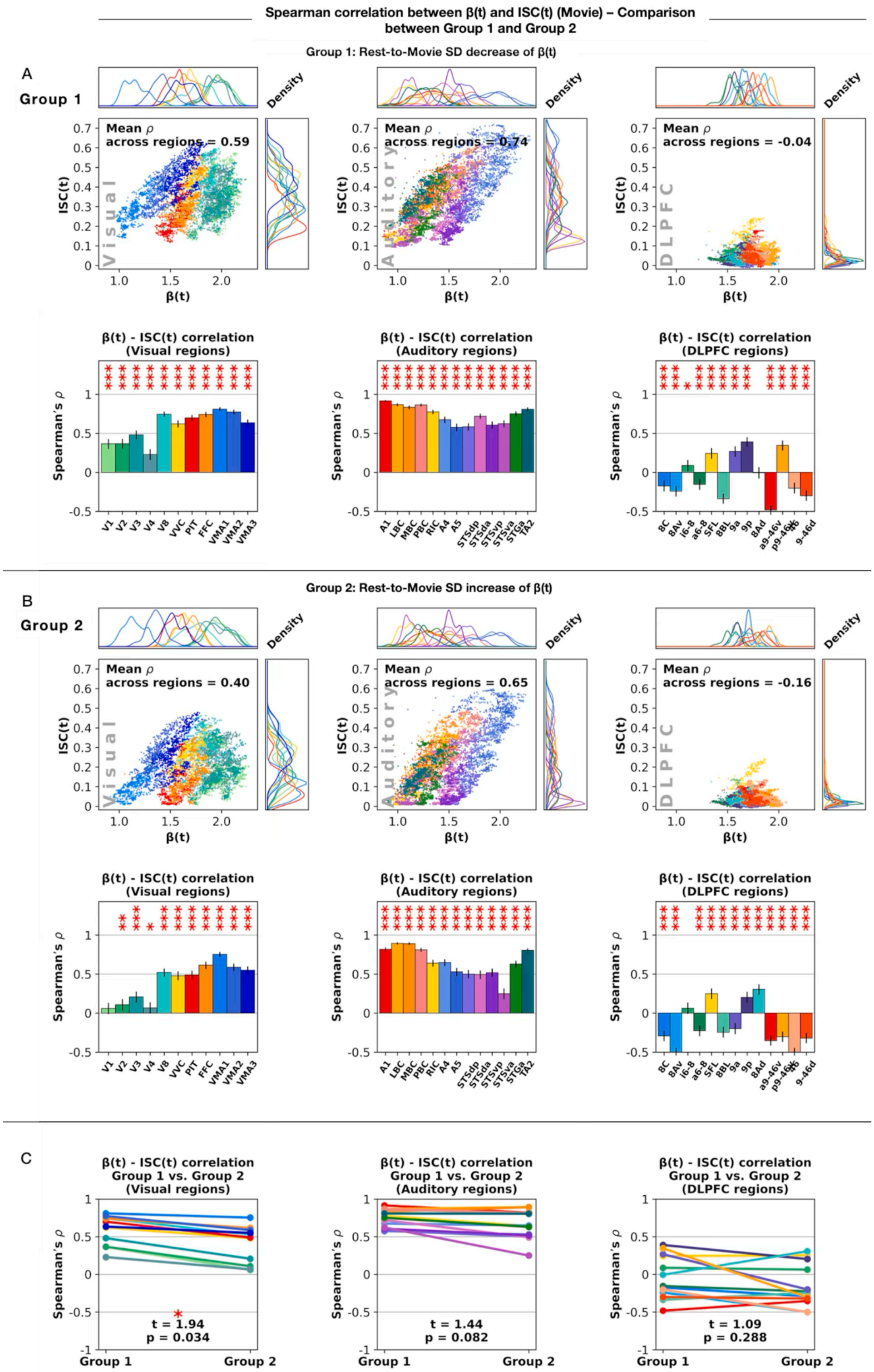

Fig. 8. Spearman's rank correlation between β(t) and ISC(t) in the MOVIE2 run in two groups. We correlated the windows of β(t) with the windows of ISC(t) in every region. Every data point in the scatterplots represents one window or data point of β(t) and ISC(t). a) β(t)-ISC(t) correlation in Group 1. b) β(t)-ISC(t) correlation in Group 2. c) Independent *t*-tests between Group 1 and Group 2 in visual, auditory, and DLPFC regions. (significance asterisks $p < 0.05$ *, $p < 0.01$ **, $p < 0.001$ ***, p-value correction = Bonferroni-Holm, error bars = 95% confidence interval).

resulting in a significant negative rather than a positive β(t)-ISC(t) correlation.

For the third aim, we first assessed the subject-based β(t) in the movie run and observed high inter-individual differences in the SD of β(t), shown in Figure 5 and in Supplementary Figures 7 and 8. Previous studies showed that the brain's spontaneous activity often interacts in a non-additive fashion with inputs to impact stimulus-induced activity (Sadaghiani et al., 2009; He, 2013; Huang et al., 2017; Podvalny et al., 2019; Northoff et al., 2024). We then asked whether the brain's relative Rest-to-Movie SD change, that is, a decrease or increase from the resting- to the movie-state, modulates ISC(t) during the movie via the formation of two subject groups (Song et al., 2021; Jangraw et al., 2023) based on the Rest-to-Movie SD change in scale-free dynamics.

We grouped subjects with Rest-to-Movie SD decrease of β(t) into Group 1 and subjects with an increase in Group 2 and then individually measured the mean of ISC(t). The two groups indeed yielded very different degrees of ISC during the movie's inputs, with Group 1 showing significantly higher ISC in visual and auditory regions than Group 2 in the three assessed movie runs, with the only exception for the auditory regions in MOVIE3. A possible theoretical inference is that higher degrees of variability in intrinsic (resting-state) scale-free dynamics only must reduce or dampen their fluctuations to support a higher impact by external inputs, thus increasing ISC when brain dynamics are less driven by intrinsic dynamics and more strongly shaped by external input dynamics (Simony et al. 2016). Although accounting for event-related designs, fMRI (Huang et al., 2017) and electrophysiological (White et al., 2012; Ito et al., 2020; Wolff et al., 2021) also provided evidence that higher degrees of pre-stimulus activity result in higher trial-to-trial variability quenching during inputs that, in turn, correlated with better stimulus processing and task performance (see also Northoff et al., 2024 for a review).

Finally, we aimed to strengthen the evidence that the brain's relative Rest-to-Movie SD change in scale-free dynamics modulates the level or mean of ISC during the movie state. First, note that we demonstrated that Group 1 (Rest-to-Movie SD decrease of β(t)) showed a significantly higher mean of ISC(t) during naturalistic inputs. Second, Group 1 also had a significantly higher positive β(t)-ISC(t) correlation in visual and auditory regions than Group 2. We infer that the higher β(t)-ISC(t) correlation in Group 1 relates to the initially observed higher mean of β(t) during naturalistic inputs than in the resting-state in the analysis of aim one: as previously discussed, higher spectral exponents induce a shift of power away from faster to slower frequencies to support higher degrees of temporal input integration during the processing of continuous inputs (Honey et al., 2012; Hasson et al., 2015; Borges et al., 2018; Wolff et al., 2022; Northoff et al., 2023). Group 1 employed a higher shift towards steeper spectral exponents and thus temporal integration of continuous inputs, thus allowing a better imprinting of the movie's audiovisual properties on brain dynamics in these subjects, finally leading to higher levels of ISC(t) and a better β(t)-ISC(t) correlation than in Group 2.

4.1. Limitations

We subsequently discuss the limitations of our study. First, we discuss a seeming contradiction between the results shown in Fig. 2 and the results shown in Fig. 7. The SD of the region-based β(t) is significantly higher in the movie run than in the resting-state for all subjects. We argued that the β(t)'s higher SD during the movie run results based on the likely ever-changing β(t) of the movie's auditory and visual inputs. At the same time, Group 1 (Rest-to-Movie SD decrease of the β(t)) has a significantly higher mean of ISC(t) during the movie run than Group 2 (Rest-to-Movie SD increase of the β(t)), as shown in Fig. 7. A question thus arises: why does Group 1 with a SD decrease yield higher ISC than Group 2 with a SD increase? We offer the following explanation of these seemingly contradicting findings. First, on the subject-based level, subjects show very different temporal structures of the β(t) in the resting-state, as paradigmatically shown for four subjects in Fig. 6b. We thus obtain a relatively flat or stable β(t) when taking the region-based mean across subjects in the resting-state. The relatively flat β(t) partially results because higher and lower β values across time generally lack an overlap across the subjects, thus resulting in a rather flat β(t) on the region-based level. Second, in the movie run, the temporal structure of the β(t) is likely more similar across subjects due to constantly shared audiovisual inputs since subjects all watched the same movie clips. The shared temporal structure of β(t) during the movie run is thus not canceled out in the averaging (region-based) process across subjects as in the resting-state, therefore yielding a distinct temporal structure of the region-based β(t) individually for each of the three assessed movie runs, as shown in Fig. 2 and Supplementary Figure 1.

How can we address that the two groups, (Rest-to-Movie SD decrease versus increase in scale-free dynamics) exhibited significantly different degrees of ISC(t) in visual and auditory regions in the movie condition? A comprehensive model that fully explains the significance of the variance of the dynamic PLE is necessary for a complete interpretation. However, we can still formulate some hypotheses based on existing frameworks and findings.

Recently, a framework addressing the dynamic repertoire of the brain, based on the number of available brain states, was proposed to explain certain phenomena, such as epilepsy (McIntosh & Jirsa, 2019; Hadriche et al., 2013). This framework prompted researchers to examine the variance in time-dependent measures of brain activity. For instance, Hudetz et al. (2015) found that the variance in time-dependent regional homogeneity (ReHo) of the BOLD signal decreases under anesthesia. Similarly, Lord et al. (2019) observed a significant reduction in the transition probabilities of recurrent patterns of leading eigenvectors derived from dynamic functional connectivity (calculated using phase-locking values) under psilocybin. In another study, Atasoy et al. (2017) discovered that the time-dependent probability distribution of connectome harmonics significantly increases with LSD. These findings suggest the importance of time-dependent variance in measurements of brain activity. Specifically, one might hypothesize that a greater availability of brain states, that is, a richer dynamic repertoire, facilitates better adaptation to external inputs. In the context of our results, an increase in variability from the resting-state to the movie state might indicate a diminished or smaller repertoire in the resting-state (than in subjects that simply had to decrease their variability in response to inputs), resulting in a relatively reduced capacity to uniformly process the movie's audiovisual inputs across subjects and consequently lower inter-subject correlation (ISC).

It is noteworthy that the spectral exponent β, measured in the frequency-domain, corresponds to other measurements, such as the Hurst exponent (H) in the time-domain. The Hurst exponent captures long-range temporal correlations (LRTCs). Temporal correlations of a signal that refer to repeating patterns in the time-series, where earlier data points can either positively or negatively correlate with later data points, across both short and long timescales (Hardstone et al., 2012). A Hurst exponent greater than 0.5 indicates persistent behavior, meaning that an increase in the value at a given time is likely to be followed by another increase, and a decrease by another decrease. A time-series with $H > 0.5$ indicates LRTCs and may correspond to a power-law distribution in the power spectrum (Linkenkaer-Hansen et al., 2001). Conversely, a Hurst exponent less than 0.5 signifies anti-persistent behavior or anticorrelated noise, where an increase is more likely to be followed by a decrease, and vice versa, as seen in mean-reverting or oscillatory dynamics (Mandelbrot, 1999). Finally, a Hurst exponent of 0.5 indicates a time-series akin to white noise, which lacks temporal correlations, and the power spectrum exhibits $\beta = 0$, with approximately equal power across all frequencies. Why did we investigate a time-dependent spectral exponent instead of, paradigmatically, a time-dependent Hurst exponent? We raised the question of how specifically naturalistic inputs, often comprising scale-free auditory and visual dynamics (Bak, 1996; Mandelbrot, 1999; Schroeder, 2009), impact scale-free brain dynamics. We consequently chose a measurement which captures scale-free dynamics, that is, measured via the relative power distribution along the frequency band by the spectral exponent.

We refrained from measuring the spectral exponent β via the irregular resampling auto-spectral analysis (IRASA) method (Wen and Liu, 2016). The IRASA is sometimes applied in electro- and magnetoencephalography studies to separate fractal from oscillatory components due to the high alpha peak or oscillation that disrupts the otherwise scale-free spectrum in electrophysiological recordings (Wainio-Theberge et al., 2022). One problem with fMRI is that the IRASA method includes down-sampling of the signal, reducing the upper-frequency end of an already limited frequency band by half. In our case, IRASA would reduce the Nyquist frequency from 0.5 Hz to 0.25 Hz due to the 7 Tesla HCP dataset's sampling rate of 1 Hz. A reduction of the frequency band by excluding faster frequencies would have fundamentally limited the principal aim of investigating the response to quickly varying audiovisual inputs. Moreover, higher frequencies of the blood-oxygenation-level-dependet (BOLD) signal can carry meaningful information (Shirer et al., 2015; Caballero-Gaudes and Reynolds, 2017). In addition to a further frequency band limitation due to using IRASA, we already constrained the lower frequency from 0.01 Hz to 0.05 Hz for the 60-second window analysis to include at least three cycles for the lowest frequency, allowing a better estimation of power in the respective lower frequency ends. Therefore, constraining the lower and upper-frequency ends would have resulted in a significantly shortened frequency band.

Although previous fMRI studies demonstrated the usability of ISC(t) as a marker for task performance or its association with traits such as paranoia (Finn et al., 2018), assessing ISC(t) for two groups which were based on neuronal (instead of behavioral) dynamics is novel. Future studies should aim to directly investigate the movie's visual and auditory inputs in addition to brain activity. Analyzing the movie's and the brain's scale-free dynamics allows a direct investigation of how brain dynamics align with naturalistic inputs. The time-dependent approach can then be applied to the visual and auditory inputs, respectively, allowing to precisely examine to what extent brain dynamics match with input dynamics, such as within the complexity matching framework to assess the relationship between scale-free systems on neuronal and behavioral grounds (West et al., 2023; Mahmoodi et al., 2023; West, 2024). We should also note that ISC(t) does not depend solely on objective input properties that are processed similarly across subjects. Instead, shared or dissimilar brain activity also depends on how cognitively and emotionally engaging the input individually for each subject is (Nastase et al., 2019). When subjects cognitively and emotionally engage with the input, or when they show higher performance in specific tasks, they can exhibit higher ISC(t) in stimulus- or task associated brain regions than subjects with less refined capabilities or engagement (Song et al., 2021; Jangraw et al., 2023).

Another limitation is that the 7 Tesla HCP dataset lacked behavioral data or recordings. Following the above, interesting results could be obtained by linking behavioral data, such as psychological scores regarding stimulus perception or task performance, with scale-free brain dynamics and their relation to input tracking. Paradigmatically, another study using ISC(t) (Jangraw et al., 2023) demonstrated that a group with higher ISC(t) also showed better task performance than a group with lower ISC(t) (see Fig 6 in Jangraw et al., 2023). Uncovering the links between brain, psychological, and behavioral dynamics on temporal-dynamical and spatial (topographical) grounds follows the neurophenomenological approach (Klar, 2021; Northoff et al., 2023) and is striven for by the Temporo-Spatial Theory of Consciousness (TTC), where temporo-spatial dynamics reflect the so-called common currency between neuronal and psychological dynamics (Northoff and Zilio, 2022; Huang, 2023).

Finally, the term "naturalistic" when used for the kind of paradigm employed in this study, lacks a precise definition valid for various types of media or movies. A recent review on the usage of naturalistic stimuli in neuroimaging (Grall and Finn, 2022) discussed aspects of so-called naturalistic stimuli relevant to consider concerning study design and for the interpretation of the obtained brain activity results. Paradigmatically, researchers should address why the chosen stimulus, such as a movie, is really naturalistic for the specific research aim of the study. Grall and Finn (2022) correctly pointed out that naturalness is not a single dimension and that different movies or clips can induce a vastly different range of human cognitions and emotions. We consider the continuous presentation of audiovisual inputs based on movie recordings that included real-life human interactions or natural sceneries as substantially better suited to investigate time-dependent scale-free brain dynamics than event-related designs. Commonly used event-related designs lack a coherent and ongoing stimulus presentation to induce a significant time-dependent spectral exponent of brain activity.

4.2. Conclusion

How do the brain's scale-free dynamics respond to continuous, naturalistic inputs and how do scale-free dynamics modulate the level of shared brain activity across subjects? To investigate these questions, we introduced a combined measurement of both a time-dependent spectral exponent β(t) and of time-dependent ISC(t). Our fMRI study provided initial evidence that the brain's time-dependent spectral exponent modulates and positively correlates with the level of shared brain activity or ISC during naturalistic inputs. We demonstrated that the brain's relative Rest-to-Movie SD change in scale-free dynamics can support the level of ISC and thus the imprint of input on brain dynamics through a two-group approach (Simony et al. 2016; Song et al., 2021; Jangraw et al., 2023). Together, our fMRI study provides initial evidence that the brain's time-dependent spectral exponent, β(t), in auditory and visual regions is related to shared brain activity, indirectly marking the imprinting of input dynamics on brain dynamics through shared fluctuations. A future study should directly investigate the time-dependent spectral exponent of both inputs and brain activity, following the common currency approach between input, neuronal, and mental dynamics (Northoff et al. 2023; Northoff et al. 2024), that is, temporo-spatial alignment, as proposed by the Temporo-Spatial Theory of Consciousness (TTC) (Northoff et al., 2024). In brief, the TTC mechanism of temporo-spatial alignment suggests that brain dynamics in early sensory regions must align and match with input dynamics to encode environmental stimuli. This is in line with the novel complexity matching framework introduced by the biological domain of fractal physiology.

Code availability

The analysis did not use special codes, tools or packages. Codes are available in case of reasonable requests.

CRediT authorship contribution statement

Philipp Klar: Writing – review & editing, Writing – original draft, Visualization, Validation, Methodology, Investigation, Formal analysis, Conceptualization. **Yasir Çatal:** Writing – review & editing, Writing – original draft, Visualization, Validation, Methodology, Investigation, Formal analysis, Conceptualization. **Gerhard Jocham:** Writing – review & editing, Validation, Supervision. **Robert Langner:** Writing – review & editing, Validation, Supervision. **Georg Northoff:** Writing – review & editing, Validation, Supervision, Methodology, Conceptualization.

Declaration of competing interest

The authors declare no conflicts of interest.

Acknowledgments

This fMRI analysis received no grant or financial support from any funding agency.

Supplementary materials

Supplementary material associated with this article can be found, in the online version, at doi:10.1016/j.neuroimage.2025.121255.

Data availability

The dataset assessed in this study is a publicly-available and nonrestricted dataset available at https://www.humanconnectome.org/.

References

Atasoy, S., Roseman, L., Kaelen, M., Kringelbach, M.L., Deco, G., Carhart-Harris, R.L., 2017. Connectome-harmonic decomposition of human brain activity reveals dynamical repertoire re-organization under LSD. Sci. Rep. 7 (1), 17661. https://doi.org/10.1038/s41598-017-17546-0.

Bak, P., 1996. How Nature Works: The Science of Self-Organized Criticality. Springer.

Bell, A.H., Hadj-Bouziane, F., Frihauf, J.B., Tootell, R.B.H., Ungerleider, L.G., 2008. Object representations in the temporal cortex of monkeys and humans as revealed by functional magnetic resonance imaging. J. Neurophysiol. 101 (2), 688–700. https://doi.org/10.1152/jn.90657.2008.

Borges, A.F.T., Giraud, A.L., Mansvelder, H.D., Linkenkaer-Hansen, K., 2018. Scale-free amplitude modulation of neuronal oscillations tracks comprehension of accelerated speech. J. Neurosci. 38 (3), 710–722. https://doi.org/10.1523/jneurosci.1515-17.2017.

Caballero-Gaudes, C., Reynolds, R.C., 2017. Methods for cleaning the BOLD fMRI signal. Neuroimage 154, 128–149. https://doi.org/10.1016/j.neuroimage.2016.12.018.

Campbell, O.L., Weber, A.M., 2022. Monofractal analysis fo functional magnetic resonance imaging: An introductory review. Hum. Brain Mapp. 43 (8), 2693–2706. https://doi.org/10.1002/hbm.25801.

Campbell, O., Vanderwal, T., Weber, A.M., 2022. Fractal-based analysis of fMRI BOLD signal during naturalistic viewing conditions. Front. Physiol. 12, 809943. https://doi.org/10.3389/fphys.2021.809943.

Chen, G., Shin, Y.W., Taylor, P.A., Glen, D.R., Reynolds, R.C., Israel, R.B., Cox, R.W., 2016. Untangling the relatedness among correlations, part I: Nonparametric approaches to inter-subject correlation analysis at the group level. Neuroimage 142, 248–259. https://doi.org/10.1016/j.neuroimage.2016.05.023.

Cutting, J.E., Brunick, K.L., Candan, A., 2012. Perceiving event dynamics and parsing Hollywood films. J. Exp. Psychol. Hum. Percept. Perform. 38 (6), 1476–1490. https://doi.org/10.1037/a0027737.

Cutting, J.E., DeLong, J.E., Brunick, K.L., 2018. Temporal fractals in movies and mind. Cogn. Res. Princ. Implic. 3 (1), 8. https://doi.org/10.1186/s41235-018-0091-x.

Cutting, J.E., DeLong, J.E., Nothelfer, C.E., 2010. Attention and the evolution of Hollywood films. Psychol. Sci. 21 (3), 440–447. https://doi.org/10.1177/0956797610361679.

Feder, J., 1988. Fractals. Plenum Press.

Field, D.J., 1987. Relations between the statistics of natural images and the response properties of cortical cells. J. Opt. Soc. Am. a 4 (12), 2379–2394. https://doi.org/10.1364/josaa.4.002379.

Field, D.J., Graham, D.J., 2007. Statistical regularities of art images and natural scenes: spectra, sparseness and nonlinearities. Spat. Vis. 21 (1-2), 149–164. https://doi.org/10.1163/156856807782753877.

Finn, E.S., 2021. Is it time to put rest to rest? Trends. Cogn. Sci. 25 (12), 1021–1032. https://doi.org/10.1016/j.tics.2021.09.005.

Finn, E.S., Corlett, P.R., Chen, G., Bandettin, P.A., Constable, R.T., 2018. Trait paranoia shapes inter-subject synchrony in brain activity during an ambiguous social narrative. Nat. Commun. 9 (1), 2043. https://doi.org/10.1038/s41467-018-04387-2.

Finn, E.S., Bandettini, P.A., 2021. Movie-watching outperforms rest for functional connectivity-based prediction of behavior. Neuroimage 235, 117963. https://doi.org/10.1016/j.neuroimage.2021.117963.

Forsythe, A., Nadal, M., Sheehy, N., Cela-Conde, C.J., Sawey, M., 2011. Predicting beauty: fractal dimension and visual complexity in art. Br. J. Psychol. 102 (1), 49–70. https://doi.org/10.1348/000712610x498958.

Gervais, C., Boucher, L.P., Villar, G.M., Lee, U., Duclos, C., 2023. A scoping review for building a criticality-based conceptual framework of altered states of consciousness. Front. Syst. Neurosci. 17, 1085902. https://doi.org/10.3389/fnsys.2023.1085902.

Glasser, M.F., et al., 2016. A multi-modal parcellation of human cerebral cortex. Nature 536 (7615), 171–178. https://doi.org/10.1038/nature18933.

Glasser, M.F., et al., 2013. The minimal preprocessing pipelines for the Human Connectome Project. Neuroimage 80, 105–124. https://doi.org/10.1016/j.neuroimage.2013.04.127.

González-Espinoza, A., Larralde, H., Martínez-Mekler, G., Müller, M., 2017. Multiple scaling behaviour and nonlinear traits in music scores. R. Soc. Open. Sci. 4 (12), 171282. https://doi.org/10.1098/rsos.171282.

Grall, C., Finn, E.S., 2022. Leveraging the power of media to drive cognition: a media-informed approach to naturalistic neuroscience. Soc. Cogn. Affect. Neurosci. 17 (6), 598–608. https://doi.org/10.1093/scan/nsac019.

Griffanti, L., Salimi-Khorshidi, G., Beckmann, C.F., Auerbach, E.J., Douaud, G., Sexton, C. E., Zsoldos, E., Ebmeier, K.P., Filippini, N., Mackay, C.E., Moeller, S., Xu, J., Yacoub, E., Baselli, G., Ugurbil, K., Miller, K.L., Smith, S.M., 2014. ICA-based artefact removal and accelerated fMRI acquisition for improved resting state network imaging. Neuroimage 95, 232–247. https://doi.org/10.1016/j.neuroimage.2014.03.034.

Grosu, G.F., Hopp, A.V., Moca, V.V., Barzan, H., Ciuparu, A., Ercsey-Ravasz, M., Winkel, M., Linde, H., Mureșan, 2023. The fractal brain: scale-invariance in structure and dynamics. Cereb. Cortex. 33 (8), 4574–4605. https://doi.org/10.1093/cercor/bhac363.

Hadriche, A., Pezard, L., Nandrino, J.L., Ghariani, H., Kachouri, A., Jirsa, V.K., 2013. Mapping the dynamic repertoire of the resting brain. Neuroimage 78, 448–462. https://doi.org/10.1016/j.neuroimage.2013.04.041.

Hardstone, R., Poil, S.S., Schiavone, G., Jansen, R., Nikulin, V.V., Mansvelder, H.D., Linkenkaer-Hansen, K., 2012. Detrended fluctuation analysis: a scale-free view on neuronal oscillations. Front. Physiol. 3, 450. https://doi.org/10.3389/fphys.2012.00450.

Hasson, U., Chen, J., Honey, C.J., 2015. Hierarchical process memory: memory as an integral component of information processing. Trends. Cogn. Sci. 19 (6), 304–313. https://doi.org/10.1016/j.tics.2015.04.006.

Hasson, U., Malach, R., Heeger, D.J., 2010. Reliability of cortical activity during natural stimulation. Trends. Cogn. Sci. 14 (1), 40–48. https://doi.org/10.1016/j.tics.2009.10.011.

Hasson, U., Nir, Y., Levy, I., Fuhrmann, G., Malach, R., 2004. Intersubject synchronization of cortical activity during natural vision. Science (1979) 303 (5664), 1634–1640. https://doi.org/10.1126/science.1089506.

He, B.J., 2011. Scale-free properties of the functional magnetic resonance imaging signal during rest and task. J. Neurosci. 31 (39), 13786–13795. https://doi.org/10.1523/jneurosci.2111-11.2011.

He, B.J., 2013. Spontaneous and Task-Evoked Brain Activity Negatively Interact. J. Neurosci. 33 (11), 4672–4682. https://doi.org/10.1523/jneurosci.2922-12.2013.

He, B.J., Zempel, J.M., Snyder, A.Z., Raichle, M.E., 2010. The temporal structures and functional significance of scale-free brain activity. Neuron 66 (3), 353–369. https://doi.org/10.1016/j.neuron.2010.04.020.

Holm, S., 1979. A simple sequentially rejective multiple test procedure. Scand. J. Stat. 6 (2), 65–70.

Honey, C.J., Thesen, T., Donner, T.H., Silbert, L.J., Carlson, C.E., Devinsky, O., Doyle, W. K., Rubin, N., Heeger, D.J., Hasson, U., 2012. Slow cortical dynamics and the accumulation of information over long timescales. Neuron 76 (2), 423–434. https://doi.org/10.1016/j.neuron.2012.08.011.

Hsü, K.J., Hsü, A., 1991. Self-similarity of the "1/f noise" called music. Proc. Natl. Acad. Sci. u S. a 88 (8), 3507–3509. https://doi.org/10.1073/pnas.88.8.3507.

Huang, Z., 2023. Temporospatial nestedness in consciousness: an updated perspective on the temporospatial theory of consciousness. Entropy 25 (7), 1074. https://doi.org/10.3390/e25071074.

Huang, Z., Liu, X., Mashour, G.A., Hudetz, A.G., 2018. Timescales of intrinsic BOLD signal dynamics and functional connectivity in pharmacologic and neuropathologic states of unconsciousness. J. Neurosci. 38 (9), 2304–2317. https://doi.org/10.1523/jneurosci.2545-17.2018.

Huang, Z., Zhang, J., Longtin, A., Dumont, G., Duncan, N.W., Pokorny, J., Qin, P., Dai, R., Ferri, F., Weng, X., Northoff, G., 2017. Is there a nonadditive interaction between spontaneous and evoked activity? Phase-dependence and its relation to the temporal structure of scale-free brain activity. Cereb. Cortex. 27 (2), 1037–1059. https://doi.org/10.1093/cercor/bhv288.

Hudetz, A.G., Liu, X., Pillay, S., 2015. Dynamic repertoire of intrinsic brain states is reduced in propofol-induced unconsciousness. Brain Connect. 5 (1), 10–22. https://doi.org/10.1089/brain.2014.0230.

Ito, T., Brincat, S.L., Siegel, M., Mill, R.D., He, B.J., Miller, E.K., Rotstein, H.G., Cole, M. W., 2020. Task-evoked activity quenches neural correlations and variability across cortical areas. PLoS. Comput. Biol. 13 (8), e1007983. https://doi.org/10.1371/journal.pcbi.1007983.

Jangraw, D.C., Finn, E.S., Bandettini, P.A., Landi, N., Sun, H., Hoeft, F., Chen, G., Pugh, K.R., Molfese, P.J., 2023. Inter-subject correlation during long narratives reveals widespread neural correlates of reading ability. Neuroimage 282, 120390. https://doi.org/10.1016/j.neuroimage.2023.120390.

Kasagi, M., Huang, Z., Narita, K., Shitara, H., Motegi, T., Suzuki, Y., Fujihara, K., Tanabe, S., Kosaka, H., Ujita, K., Fukuda, M., Northoff, G., 2017. Association between scale-free brain dynamics and behavioral performance: functional MRI study in resting state and face processing task. Behav. Neurol. 2017, 2824615. https://doi.org/10.1155/2017/2824615.

Kauppi, J.P., Jässkeläinen, I.P., Sams, M., Tohka, J., 2010. Inter-subject correlation of brain hemodynamic responses during watching a movie: localization in space and frequency. Front. Neuroinform. 4, 5. https://doi.org/10.3389/fninf.2010.00005.

Klar, P., 2021. What is neurophilosophy: do we need a non-reductive form? Synthese 199, 2701–2725. https://doi.org/10.1007/s11229-020-02907-6.

Klar, P., Çatal, Y., Langner, R., Huang, Z., Northoff, G., 2023a. Scale-free dynamics in the core-periphery topography and task alignment decline from conscious to unconscious states. Commun. Biol. 6 (1), 499. https://doi.org/10.1038/s42003-023-04879-y.

Klar, P., Çatal, Y., Langner, R., Huang, Z., Northoff, G., 2023b. Scale-free dynamics of the core-periphery topography. Hum. Brain Mapp. 44 (5), 1997–2017. https://doi.org/10.1038/s42003-023-04879-y.

Lakatos, P., Gross, J., Thut, G., 2019. A new unifying account of the roles of neuronal entrainment. Curr. Biol. 29 (18), 890–905. https://doi.org/10.1016/j.cub.2019.07.075.

Kriegeskorte, N., et al., 2008. Matching categorical object representations in inferior temporal cortex of man and monkey. Neuron 60 (6), 1126–1141. https://doi.org/10.1016/j.neuron.2008.10.043.

Kringelbach, M.L., Sanz Perl, Y., Tagliazucchi, E., Deco, G., 2023. Toward naturalistic neuroscience: Mechanisms underlying the flattening of brain hierarchy in movie-watching compared to rest and task. Sci. Adv. 9 (2), eade6049. https://doi.org/10.1126/sciadv.ade6049.

Laumann, T.O., Snyder, A.Z., Mitra, A., Gordon, E.M., Gratton, C., Adeyemo, B., Gilmore, A.W., Nelson, S.M., Berg, J.J., Greene, D.J., McCarthy, J.E., Tagliazucchi, E., Laufs, H., Schlaggar, B.L., Dosenbach, N.U.F., Petersen, S.E., 2017. On the stability of BOLD fMRI correlations. Cereb. Cortex. 27 (10), 4719–4732. https://doi.org/10.1093/cercor/bhw265.

Levitin, D.J., Chordia, P., Menon, V., 2012. Musical rhythm spectra from Bach to Joplin obey a 1/f power law. Proc. Natl. Acad. Sci. u S. a 109 (10), 3716–3720. https://doi.org/10.1073/pnas.1113828109.

Linkenkaer-Hansen, K., Nikouline, V.V., Palva, M., Ilmoniemi, R.J., 2001. Long-range temporal correlations and scaling behavior in human brain oscillations. J. Neurosci. 21 (4), 1370–1377. https://doi.org/10.1523/JNEUROSCI.21-04-01370.2001.

Lord, L.D., Expert, P., Atasoy, S., Roseman, L., Rapuano, K., Lambiotte, R., Nutt, D.J., Deco, G., Carhart-Harris, R.L., Kringelbach, M.L., Cabral, J., 2019. Dynamical exploration of the repertoire of brain networks at rest is modulated by psilocybin. Neuroimage 199, 127–142. https://doi.org/10.1016/j.neuroimage.2019.05.060.

Luque, J., Luque, B., Lacasa, L., 2015. Scaling and universality in the human voice. J. R. Soc. Interface 12 (105), 20141344. https://doi.org/10.1098/rsif.2014.1344.

Mahmoodi, K., Kerick, S.E., Grigolini, P., Franaszczuk, P.J., West, B.J., 2023. Comβxity synchronization: a measure of interaction between the brain, heart and lungs. Sci. Rep. 13 (1), 11433. https://doi.org/10.1038/s41598-023-38622-8.

Mahmoodi, K., West, B.J., Grigolini, P., 2020. On the dynamical foundation of multifractality. Phys. A: Stat. Mech. Appl. 551, 124038. https://doi.org/10.1016/j.physa.2019.124038.

Mandelbrot, B.B., 1999. Multifractals and 1/f Noise. Wild Self-Affinity in Physics. Springer.

McIntosh, A.R., Jirsa, V.K., 2019. The hidden repertoire of brain dynamics and dysfunction. Netw. Neurosci. 3 (4), 994–1008. https://doi.org/10.1162/netn_a_00107.

Nastase, S.A., Gazzola, V., Hasson, U., Keysers, C., 2019. Measuring shared responses across subjects using intersubject correlation. Soc. Cogn. Affect. Neurosci. 14 (6), 667–885. https://doi.org/10.1093/scan/nsz037.

Neyman, J., 1937. Outline of a theory of statistical estimation based on the classical theory of probability. Phil. Trans. R. S. London, Ser. A, No. 767 236, 333–380.

Northoff, G., Klar, P., Bein, M., Safron, A., 2023. As without, so within: how the brain's temporo-spatial alignment to the environment shapes consciousness. Interface Focus. 13 (3), 20220076. https://doi.org/10.1098/rsfs.2022.0076.

Northoff, G., Zilio, F., 2022. Temporo-spatial Theory of Consciousness (TTC) - bridging the gap of neuronal activity and phenomenal states. Behav. Brain Res. 424, 113788. https://doi.org/10.1016/j.bbr.2022.113788.

Northoff, G., Zilio, F., Zhang, J., 2024. Beyond task response-Pre-stimulus activity modulates contents of consciousness. Phys. Life Rev. 49, 19–37. https://doi.org/10.1016/j.plrev.2024.03.002.

Nguyen, M., Chang, A., Micciche, E., Meshulam, M., Nastase, S.A., Hasson, U., 2022. Teacher-student neural coupling during teaching and learning. Soc. Cogn. Affect. Neurosci. 17 (4), 367–376. https://doi.org/10.1093/scan/nsab103.

Nyikos, L., Balázs, L., Schiller, R., 1994. Fractal analysis of artistic images: from cubism to fractalism. Fractals. 2 (1), 143–152. https://doi.org/10.1142/S0218348X94000144.

Pelekanos, V., Mur, M., Storrs, K.R., 2016. Extracting object identity: ventral or dorsal visual stream? J. Neurosci. 36 (24), 6368–6370. https://doi.org/10.1523/JNEUROSCI.1102-16.2016.

Podvalny, E., Flounders, M.W., King, L.E., Holroyd, T., He, B.J., 2019. A dual role of prestimulus spontaneous neural activity in visual object recognition. Nat. Commun. 10 (1), 3910. https://doi.org/10.1038/s41467-019-11877-4.

Rolls, E.T., Deco, G., Huang, C.C., Feng, J., 2023b. Multiβ cortical visual streams in humans. Cereb. Cortex. 33 (7), 3319–3349. https://doi.org/10.1093/cercor/bhac276.

Rolls, E.T., Deco, G., Huang, C.C., Feng, J., 2022. The human language effective connectome. Neuroimage 258, 119352. https://doi.org/10.1016/j.neuroimage.2022.119352.

Rolls, E.T., Rauschecker, J.P., Deco, G., Huang, C.C., Feng, J., 2023a. Auditory cortical connectivity in humans. Cereb. Cortex. 33 (10), 6207–6227. https://doi.org/10.1093/cercor/bhac496.

Sabanal, S., Nakagawa, M., 1996. The fractal properties of vocal sounds and their application in the speech recognition model. Chaos, Solit. Fract. 7 (11), 1825–1843. https://doi.org/10.1016/S0960-0779(96)00043-4. https://ui.adsabs.harvard.edu/link_gateway/1996CSF.....7.1825S/.

Sadaghiani, S., Hesselmann, G., Kleinschmidt, A., 2009. Distributed and antagonistic contributions of ongoing activity fluctuations to auditory stimulus detection. J. Neurosci. 29 (42), 13410–13417. https://doi.org/10.1523/jneurosci.2592-09.2009.

Salimi-Khorshidi, G., Douaud, G., Beckmann, C.F., Glasser, M.F., Griffanti, L., Smith, S. M., 2014. Automatic denoising of functional MRI data: combining independent component analysis and hierarchical fusion of classifiers. Neuroimage 90, 449–468. https://doi.org/10.1016/j.neuroimage.2013.11.046.

Schroeder, M., 2009. Fractals, Chaos, Power Laws: Minutes from an Infinite Paradise. Dover Publications.

Shirer, W.R., Jiang, H., Price, C.M., Ng, Bernard, Greicius, M.D, 2015. Optimization of rs-fMRI pre-processing for enhanced signal-noise separation, test-retest reliability, and group discrimination. Neuroimage 117, 67–79. https://doi.org/10.1016/j.neuroimage.2015.05.015.

Siegel, A.F., 1982. Robust regression using repeated medians. Biometrika 69, 242–244. https://doi.org/10.1093/biomet/69.1.242.

Simony, E., Honey, C.J., Chen, J., Lositsky, O., Yeshurun, Y., Wiesel, A., Hasson, U., 2016. Dynamic reconfiguration of the default mode network during narrative comprehension. Nat. Commun. 7, 12141. https://doi.org/10.1038/ncomms12141.

Song, H., Finn, E.S., Rosenberg, M.D., 2021. Neural signatures of attentional engagement during narratives and its consequences for event memory. Proc. Natl. Acad. Sci. USA 118 (33), e2021905118. https://doi.org/10.1073/pnas.2021905118.

Sonkusare, S., Breakspear, M., Guo, C., 2019. Naturalistic stimuli in neuroscience: critically acclaimed. Trends. Cogn. Sci. 23 (8), 699–714. https://doi.org/10.1016/j.tics.2019.05.004.

Su, Z.Y., Wu, T., 2007. Music walk, fractal geometry in music. Phys. A: Stat. Mech. Appl. 380, 418–428. https://doi.org/10.1016/j.physa.2007.02.079.

Tagliazucchi, E., Chialvo, D.R., Siniatchkin, M., Amico, E., Brichant, J.F., Bonhomme, V., Noirhomme, Q., Laufs, H., Laureys, S., 2016. Large-scale signatures of unconsciousness are consistent with a departure from critical dynamics. J. R. Soc. Interface 114, 20151027. https://doi.org/10.1098/rsif.2015.1027.

Van Essen, D.C., Smith, S.M., Barch, D.M., Behrens, T.E.J., Yacoub, E., Ugurbil, K., 2013. The WU-Minn human connectome project: an overview. Neuroimage 80, 62–70. https://doi.org/10.1016/j.neuroimage.2013.05.041.

Voss, R.F., Clarke, J., 1978. 1/f noise" in music: Music from 1/f noise. J. Acoust. Soc. Am. 63, 258–263. https://doi.org/10.1121/1.381721.

Voss, R.F., Clarke, J., 1975. 1/f noise in music and speech. Nature 258, 317–318. https://doi.org/10.1038/258317a0.

Wainio-Theberge, S., Wolff, A., Gomez-Pilar, J., Zhang, J., Northoff, G., 2022. Variability and task-responsiveness of electrophysiological dynamics: Scale-free stability and oscillatory flexibility. Neuroimage 256, 119245. https://doi.org/10.1016/j.neuroimage.2022.119245.

Wen, H., Liu, Z., 2016. Separating fractal and oscillatory components in the power spectrum of neurophysiological signal. Brain Topogr. 29, 13–26. https://doi.org/10.1007/s10548-015-0448-0.

West, B.J., 2024. Comβxity synchronization in living matter: a mini review. Front. Netw. Physiol. 4, 1379892. https://doi.org/10.3389/fnetp.2024.1379892.

West, B.J., Grigolini, P., Kerick, S.E., Franaszczuk, P.J., Mahmoodi, K., 2023. Comβxity Synchronization of Organ Networks. Entropy. (Basel) 25 (10), 1393. https://doi.org/10.3390/e25101393.

White, B., Abbott, L.F., Fiser, J., 2012. Suppression of cortical neural variability is stimulus- and state-dependent. J. Neurophysiol. 108, 2383–2392. https://doi.org/10.1152/jn.00723.2011.

Wolff, A., Berberian, N., Golesorkhi, M., Gomez-Pilar, J., Zilio, F., Northoff, G., 2022. Intrinsic neural timescales: temporal integration and segregation. Trends. Cogn. Sci. 26 (2), 159–173. https://doi.org/10.1016/j.tics.2021.11.007.

Wolff, A., Chen, L., Tumati, S., Golesorkhi, M., Gomez-Pilar, J., Hu, J., Jiang, S., Mao, Y., Longtin, A., Northoff, G., 2021. Prestimulus dynamics blend with the stimulus in neural variability quenching. Neuroimage 238, 118160. https://doi.org/10.1016/j.neuroimage.2021.118160.